Nemzeti Tehetség Program

Scientific, Technical and Art Releases – 2020

Scientific, Technical and

Art Releases – 2020

Publisher:
Media Technology and Light Industry Institute of
Rejtő Sándor Faculty of Light Industry and
Environmental Engineering
Óbuda University

Editor-in-Chief:
Dr. Edit Csanák

Reader Editor:
Dr. Edit Csanák

Technical Editor:
Piroska Prokai

Printed in Budapest by
ÓE RKK MKI Digital Printing Office

The publication is made in 150 copies in A5 volume
ISBN 978-963-449-228-3

TABLE OF CONTENTS

MONITORING OF THE KEROSENE AND CADMIUM CONTAMINATED SOIL NEAR THE AIRPORT

Ágnes BÁLINT, Glória BELNVALNER, Bernadett GYARMATI

Abstract: *It is well-known that the aviation industry releases dangerous chemicals into the air. The caused damage is often evident on a local level, as the herbage's dilapidated state indicates pollution clearly. Aviation related damage was found in the acacia forest next to the Airport, Budapest; therefore, kerosene and cadmium load of the soil was examined. Kerosene content reached 0.99 g in 10 g soil, and the average cadmium contamination was 14.12 ±2.50 mg kg-1 dry matter.*

Keywords: *Cadmium; Kerosene; Pollution; Soil*

INTRODUCTION

Environmental risks of cadmium contamination

Release of cadmium (Cd) into the environment is connected predominantly to the auto and aerospace industry, stabilization of polyvinylchloride, manufacture of batteries, etc. Moreover, some phosphate fertilizers have been found to contain high levels of Cd [1]. Cd released into the environment tends to concentrate in soils and sediments, thereby creating chances to enter into the food-chain via rooted plants. Cd toxicity is well documented [2]: kidney and liver represent the principal target organs for Cd accumulation in mammals [3], and a wide range of pathological effects on fish and other aquatic organisms have been reported as well [4]. Since humans ingest Cd in higher amounts from edible plants (primarily cereals) than from meat, there is a well-founded need to extend our knowledge on Cd uptake in soil/plant interaction.

Although Cd contamination in soil and/or in plants has been investigated for a long time [5] it still deserves attention as a research topic due to its complexity [6]. Characteristics of the environment have an enormous impact on bioavailability. In the case of soil, the structure, the texture, the pH, and the organic matter content have crucial importance on uptake control and availability [7], thereby on the level of toxicity. It has been confirmed by several studies that there is a linear correlation between soil pH and Cd uptake by plants [8].

MATERIALS AND METHODS

Soil sampling and preparation

In the frame of a comprehensive survey on heavy metal pollution (Cd, Zn, Cu, Fe, Mn, Pb), 18 spot samples (labeled SPOT 1–18) and 9 control samples (labeled CTRLC1–9) were collected at a depth of 0-30 cm, on the area with extensive damage to acacia (approximately 7500 m^2), in front of the terminal of the Airport (outside the fence, Budapest, Hungary).

The size of the control area was approximately 40000 m^2. Before the sample taking, the control area was supposedly Cd and kerosene free.

Samples were taken according to the sampling network based on ISO 10381-2:2002 standards (Figure 1.).

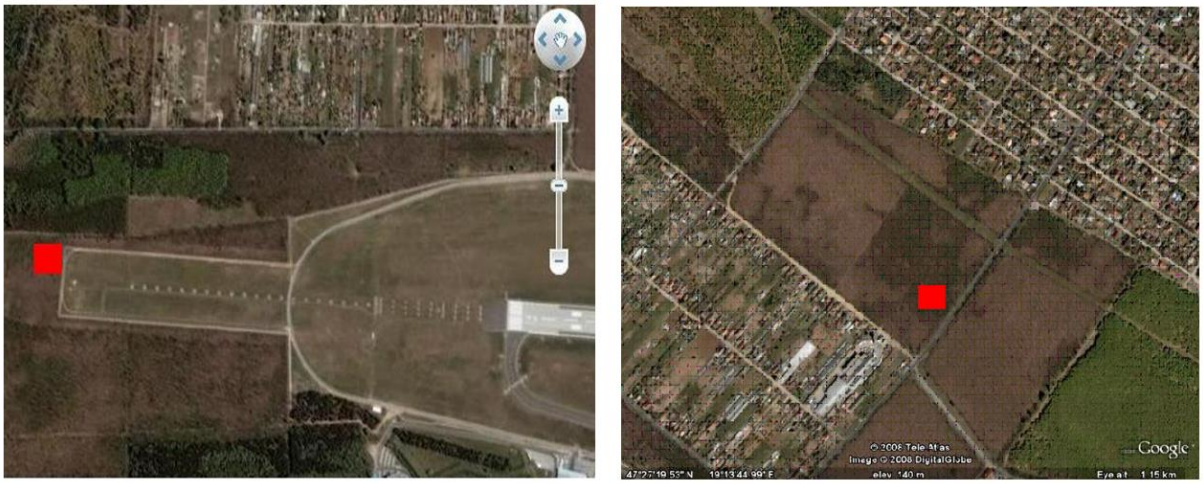

Figure 1: The heavy metal contamination of the soil was tested beside runway Ferihegy I. (left: with a red spot, where cadmium and kerosene pollutions were found; right: with another red spot, where control samples were taken)

Samples were left to dry by exposure to air. To remove the bigger stones and root remnants, the samples were sieved through a 2 mm stainless steel sieve.

Dry weight content was determined according to ISO 11465:1993 standards.

Compensation calculation procedure:

$$n = (a - b) / a * 100,$$

where:

n = the dry matter content of air-dry soil, %
a = the mass of the air-dry soil (g)
b = the mass of the soil after drying, (g)

The pH_{KCl} of samples were measured by Radelkis OP-211 pH-meter according to ISO 10390:2005 standard. The importance of soil pH in bioavailability is confirmed by several authors [14].

To determine kerosene 10-10 g soil samples were weighed by analytical balance and put into glass vials, then 20 cm^3 of methanol (96% HPLC grade, Lab-Scan) was added. Samples were placed for 10 minutes into an Ultrasonic Bath (Transsonic T 460, Elma), after which they were filtered through a 0.45 μm membrane filter (Millipore, Cat. No. HAWP04700) twice. 0.6 cm^3 of liquid was taken out and 6 cm^3 of distilled water (HPLC grade) was added to it. The kerosene

content was determined by GC-MS (GC Agilent Typ. 7890A.; MS Agilent Typ. 5975 C. Ionsource: 250 C, ionization energy: 70 eV interface: 250 C) in the laboratory of Kromat Ltd., Eötvös Roland University.

To determine the pseudo total Cd content, samples were digested by a MILESTONE 1200 Mega Microwave Digestion Oven described in Table 1.

Table 1. Digestion program for soil samples

Steps	Period of time	Efficiency
	minutes	W
1.	0:05:00	250
2.	0:02:00	0
3.	0:05:00	400
4.	0:05:00	250
5.	0:07:00	700
Ventillation: 00:05:00 Rotorctrl: on Twist: on		

After the procedure described above, the pseudo total Cd content was measured by ATI 939 UNICAM FAAS in soil.

For the digestion, samples were sieved through a 0.2mm stainless-steel sieve. 0.5 g dry matter soil was put into each bomb. Then 5 cm^3 of 65% HNO_3 (analytical grade, Thomasker Finechemicals Company) and 2 cm^3 of 30% H_2O_2 (analytical grade, Thomasker Finechemicals Company) were added and let to stay in the solution for half an hour and then put the bombs into the microwave oven for half an hour. After that, the bombs were put into water cooling for half an hour, and when they cooled, they were opened under a fume hood. The suspension made was filtered into 25 cm^3 standard flask, then it was filled up with high purity distilled water. The samples were stored in a refrigerator until the instrument measuring. The digestion was done according to the „Cook-book" recipe of Milestone mega 12000 microwave oven. Table 1. contains the recipe of digestion in a microwave oven.

Statistical evaluation

Data obtained were subjected to ANOVA. The statistical calculations were performed by SPSS 14.0 software package.

RESULTS AND DISCUSSION

Pseudo total Cd content of soil derived from area close to Budapest airport

Cd was the only element among the other measured heavy metals with outstanding concentration compared to regulation limit. The average of the pseudo total Cd content of samples was 14.12 ±2.50 mg kg^{-1} dry matter, which greatly exceeds the average (1–2.5 mg kg^{-1} d. m., dry matter) regulation limit of the countries in the European Union. Figure 2. denotes the pseudo total cadmium pollution of SPOT1-18.

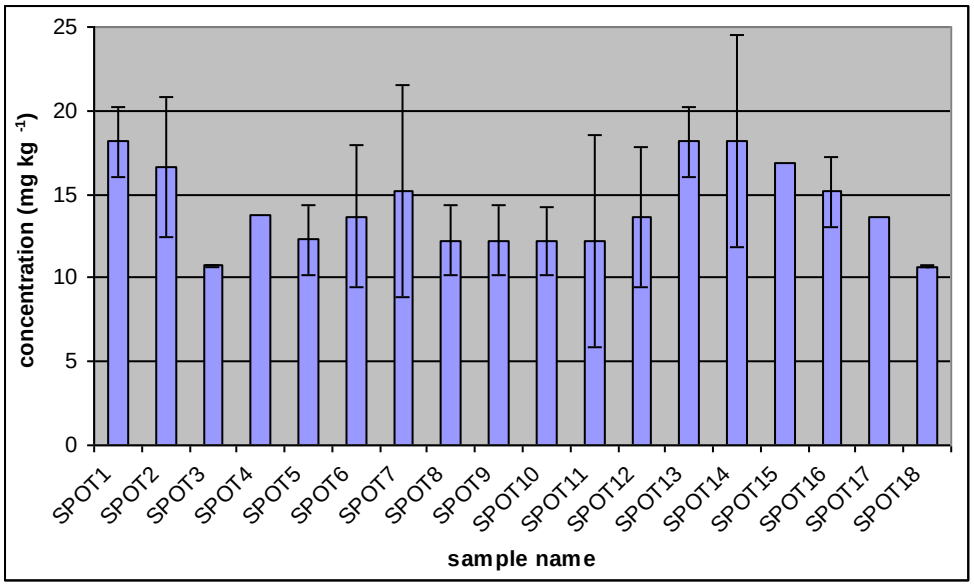

Figure 2: The cadmium concentration (mg kg^{-1}) in SPOT samples next to the Airport, Budapest

The average soil SPOT1-18 contained 0.99 g kerosene 10 g-1 soil sample (Figure 3.)

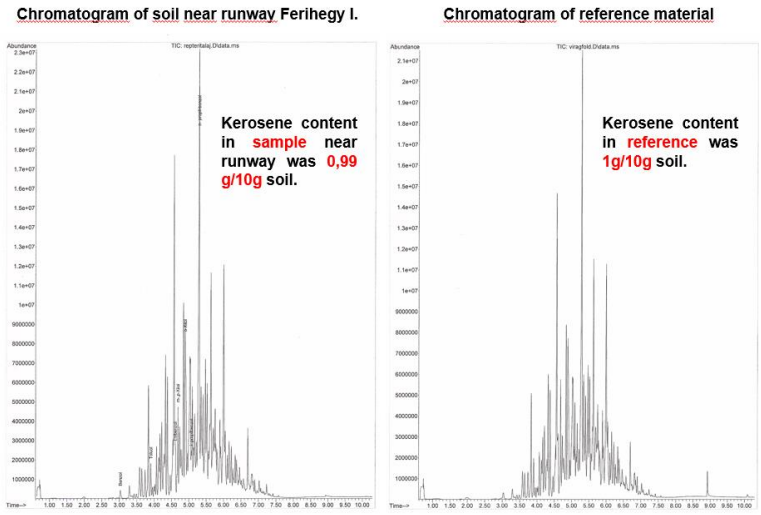

Figure 3: Determination of kerosene in soil samples by GC-MS (Agilent) SHS (static headspace gas chromatographic method) method

The average pH of the soil varies 5.27-7.84 (polluted soil) and 4.53-7.60 (control soil) in the case of pH_{KCl}. In most cases, acidic pH was measured, which assists the Cd mobilization causing the inhibition of growth and photosynthesis of plants. Furthermore, it hinders the uptake and transport of essential micro elements (Fe, Cu, Zn) [15], etc.

CONCLUSIONS

A cadmium and kerosene polluted area was detected next to the airport (former Ferihegy I.) of Budapest, Hungary. Creation and execution of a remediation plan is a major task to reduce the

soil load originating from airport operations and to stop further distribution of the pollutants. Therefore, regular area monitoring of the pollutant could give a solid base for the organisation of remediation tasks.

ACKNOWLEDGEMENTS

B. Gyarmati wishes to thank Helmholtz Centre for Environmental Research – UFZ. The authors are grateful to K. Torkos for his valuable help and G. Gyulai, A. Gyarmati, and J. M. Dedon for the draft manuscript's critical comments.

REFERENCES

[1] Ulrich, A. E. (2019): *Cadmium governance in Europe's phosphate fertilizers: Not so fast?,* Science of The Total Environment, 650(1), p541-545
[2] Khafaga, A. F. et al. (2019): *The potential modulatory role of herbal additives against Cd toxicity in human, animal, and poultry: a review*, Environmental Science and Pollution Research, 26, p4588–4604
[3] Jurczuk, M. et al. (2004): *Antioxidant enzymes activity and lipid peroxidation in liver and kidney of rats exposed to cadmium and ethanol*, Food and Chemical Toxicology, 42, p429-438
[4] Hashim, E. S. H. – Al-Yassein, R. N. (2020): *Effect of Sublethal Concentrations of Cadmium on the Histo-pathological Changes of Muscles of Planiliza abu Juveniles (Heckel, 1843),* Basrah J. Agric. Sci., 33(2), p207-217
[5] Fajardo, C. et al. (2019): *Pb, Cd, and Zn soil contamination: Monitoring functional and structural impacts on the microbiome,* Applied Soil Ecology, 135, p56-64
[6] Hamid, Y. et al., (2020): *Cadmium mobility in three contaminated soils amended with different additives as evaluated by dynamic flow-through experiments,* Chemosphere, 261, p127763
[7] Kirkham, M. B. (2006): *Cadmium in plants on polluted soils: Effects of soil factors, hyperaccumulation, and amendments*, Geoderma, 137, p19-32
[8] He, H. et al. (2017): *Growth and Cd uptake by rice (Oryza sativa) in acidic and Cd-contaminated paddy soils amended with steel slag,* Chemosphere, 189, p247-254
[9] Kumar, D. - Kim, C. J. (2019): *New insights into bioremediation strategies for oil-contaminated soil in cold environments*, International Biodeterioration & Biodegradation, 142, p58-72
[10] Mattie, D. R. et al. (2018): *Toxicity and occupational exposure assessment for Fischer-Tropsch synthetic paraffinic kerosene*, Journal of Toxicology and Environmental Health, Part A, 81(16), p774-791
[11] Mattie, R. D. (2020): *Toxicity and human health assessment of an alcohol-to-jet (ATJ) synthetic kerosene*, Journal of Toxicology and Environmental Health, Part A, 83(21-22), p687-701
[12] Collins, C. (2007): *Implementing Phytoremediation of Petroleum Hydrocarbons, Phytoremediation.* Methods in Biotechnology, 23 (1), p99-108
[13] Adipah, S. (2019): *Introduction of Petroleum Hydrocarbons Contaminants and its Human Effects,* Journal of Environmental Science and Public Health, 3(1), p001-009
[14] Adams, M. L. et al. (2004): *Predicting Cadmium Concentration in Wheat and Barley Grain Using Soil Properties*, Journal of Environmental Quality, 33, p532-541
[15] Yang, L. et al. (2020): *Bioavailability of cadmium to celery (Apium graveolens L.) grown in acidic and Cd-contaminated greenhouse soil as affected by the application of hydroxyapatite with different particle sizes,* Chemosphere, 240, p124916, 1-9

COLOR CHANGES DURING THE PRODUCTION OF LAMINATED FLEXOGRAPHIC PRINTS

Kristóf CZIMBALMOS, Ákos BORBÉLY

Abstract: *Lamination causes observable changes in the visual appearance of prints. As a common surface finishing procedure, lamination produces a product with improved physical properties, but the resulting optical changes often challenge accurate color reproduction. The prediction of the color appearance of the final product is made difficult because the laminated product has a complex multi-layer optical system that can not be described by the combination of the effects of the individual layers. In this study, we examined the shifts of colorimetric properties caused by the lamination of flexographic prints. In our experiment, 31 color centers were measured before the lamination and after the process. We also investigated the accuracy of a practical simulation method that uses water in place of the adhesive.*

Keywords*: flexographic printing, lamination, standard illuminant, color measurement*

INTRODUCTION

Flexography is the dominant printing technology of the packaging sector; with the flexible printing form, excellent print quality can be achieved on a whole range of printing substrates.

The ever-growing market competition requires the use of additional technologies to produce high-quality packaging materials. By lamination technology, beneficial features of various raw materials can be added, thus creating a multi-layer material for many areas of application. From the aspect of printing technologies, it is beneficial that the print itself can be enclosed between two layers enabling the material to meet more rigorous requirements of different industries in addition to the enhanced appearance. *In packaging, lamination is also used to improve the barrier properties of substrates. The end-use of the product will determine the choice of the most suitable laminating process;* many different technologies are available.

The successful application of laminate over the inked surface depends on many factors. The ink needs to be completely dry, not only on the surface; otherwise, the lamination process may result in undesired anomalies that affect the plastic film, causing the film to detach and making the printed sheet a waste product. It is inevitable to compare the colors of the printed and the non-laminated copy. The laminate that is put down directly on the printed sheet will cause variation in the path of the light passing through the plastic film before and after the interaction with the print. The outcome of this complex optical modification will be perceivable to a human observer. For example, a parameter that will suffer significant alteration (increase) on a laminated printed sheet relative to a non-laminated one is tone value. The main factor determining tone value increase is the optical behavior of the printed substrate; the film layer may further amplify the visual perception of the dot dimensions. This may cause the contrast and intensity of the colors change at an unwanted rate. In this study, we examined how lamination alters the color properties of flexographic prints.

EXPERIMENTAL PART

The flexograpic prints were produced on a Windmöller & Hölscher Miraflex wide-web press. The lamination was accomplished by a Nordmeccanica Super Combi 4000 coating unit with vectorial drive motors and web tension control. This unit can use both water-based and solvent-based adhesives. (figure 1) Most of the products were created using solventless adhesives. Solventless technology has recently improved to be applicable in lamination processes with flexible packaging films.[1]

The substrates were BOPP and PET foils of 12-25 μm thickness. The laminating foil was PE and BOPP with 30-80 μm thickness. Both front side and backside prints were involved in the investigation. Some of the prints had white underprint (on the transparent substrate), which was taken into consideration during the measurements.

Figure 1: FWindmöller & Hölscher Miraflex flexographic press[2] (left) and Nordmeccanica Super Combi 4000 coating unit[3] (right)

The products were measured at three different stages. First, the laminate was imposed on the print. After that, water was sprayed between the two layers; this practical way of simulating the final product is applied as a custom procedure in some printing houses (e.g., where the test prints were produced). Last, the laminated print was measured.

Measurements were carried out on the white background, with an X-Rite eXact Standard type instrument set to M3 standard (ISO 13655, measurement with polarization filter) mode. The average repeatability of the measurements was 0.4 ΔE^*_{ab}. Tristimulus values were obtained with both D65 and D50 standard illuminants (figure 2). While D65 is considered average daylight, recommended by the CIE[4] (International Commission on Illumination) and widely used in the graphic industry, D50 is recommended by the ICC (International Color Consortium) for the white point of the profile connections space for standard color management[5].

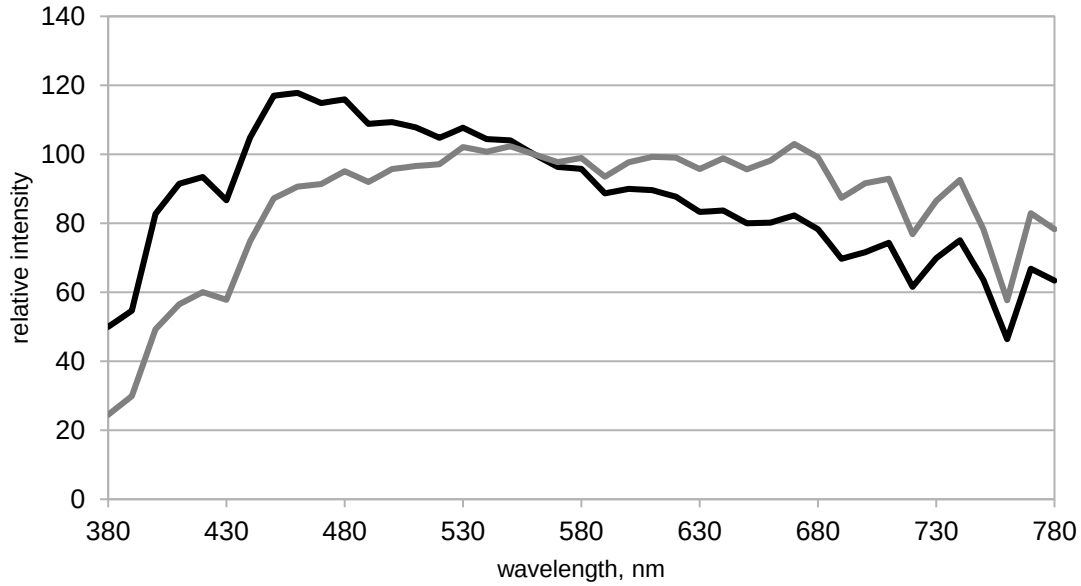

Figure 2: Relative spectral power distributions of CIE standard illuminants[4] D65 (solid, black) and D50 (dashed, grey).

RESULTS

In this study, 31 color centers were examined; they were selected from the layout of the running jobs. First, the effect of lamination was tested, by measuring the color differences between color centers prior to the lamination, with the foil superimposed and the final product (table 1).

Table 1: Color differences (ΔE^*_{ab}) between the print with the laminate superimposed and the final product under D50 and D65 standard illuminants

Specimen	D50	D65
Average of all	5.1	5.4
No underprint	8.4	9
Underprinted	1.8	1.7

The values indicate that the average color differences are large, well visible. However, if the values of the underprinted samples are separated from the other products (shown in the last two rows of table 1, 2, and 3), the group of the latter exhibits almost twice as large differences, while the average of the rest is not far from the threshold visibility.

The subjects of the second comparison were the flexographic print with the laminate superimposed and the same setup with water sprayed between the layers to provide a higher refractive index medium. Results are presented in table 2.

Table 2: Color differences (ΔE^*_{ab}) between the print with the laminate superimposed and the same with water sprayed in between, under D50 and D65 standard illuminants

Specimen	D50	D65
Average of all	3.3	3.6
No underprint	5.3	5.9
Underprinted	1.3	1.2

Table data represent smaller color shifts than in the previous case. The water spraying method meant to simulate the final product. This method will alter the visual appearance significantly, but less than the real process. The effectiveness of the simulation can be expressed by the comparison of the water sprayed and the final product (table 3).

Table 3: Color differences (ΔE^*_{ab}) between the water sprayed simulation and the final product under D50 and D65 standard illuminants

Specimen	D50	D65
Average of all	2.6	2.7
No underprint	3.4	3.6
Underprinted	1.9	1.8

These values confirm that the visual difference between the "water laminated" samples and the final product is in the well visible range.

The choice of the standard illuminant (D50 and D65) had no significant influence on the results; only the fraction of the unit (just noticeable) color difference can be observed between the values obtained with the two illuminants. As a further evaluation, we examined the lightness (ΔL^*) and chroma (ΔC^*_{ab}) components of the color differences, as shown in table 4.

Table 4: Lightness (ΔL^*) and chroma (ΔC^*_{ab}) differences between the print with the laminate superimposed and the final product under D65 standard illuminant

Specimen	ΔL^*	ΔC^*_{ab}
Average of all	2.7	4.3
No underprint	5.2	7.8
Underprinted	1.1	1.9

In this case (comparison of the print with the laminate superimposed and the final product) and in the other cases as well, we found that chroma shifts were larger than the shift in lightness.

CONCLUSIONS

In our study, we investigated the alteration of color appearance of flexographic prints caused by the lamination. We measured 31 color centers before and after the lamination and in a simulation method, where water replaced the adhesive. We found that lamination caused large, well visible color differences; underprinted samples were less affected. Chroma shifts were more responsible for the color differences than the change in lightness. The choice of the standard illuminant (D50 or D65) during the calculation of the colorimetric data had no significant influence on the color difference values. Our results have shown that spraying water between the print and the foil as the adhesive simulation is an inaccurate representation of the final product.

REFERENCES

[1] Guo P., Fu Y., Cui X., et. al. (2019): *Preparation and Properties of PET/PE Solvent-Free Laminated Packaging Films.* In: Zhao P., Ouyang Y., Xu M., Yang L., Ren Y. (eds) *Advances in Graphic Communication, Printing and Packaging*. Lecture Notes in Electrical Engineering, vol 543. Springer, Singapore. http://doi-org-443.webvpn.fjmu.edu.cn/10.1007/978-981-13-3663-8_121

[2] Im*age:* Windmöller und Hölscher Magazin homepage https://www.wuh-lengerich.de/en/nc/units/public-relations/details/news/miraflex-the-most-successful-central-impression-ci-flexographic-printing-press-in-the-world/ (Accessed 05/12/2019)

[3] Image: Nordmeccanica Group homepage https://www.nordmeccanica.com/en/combi_solutions/combi_photogallery.php (Accessed 05/12/2019)

[4] Commission Internationale de l'Eclairage (2006): *Colorimetry — Part 2: CIE Standard Illuminants for Colorimetry* ISO 11664-2:2007(E)/CIE S 014-2/E:2006

[5] International Color Consortium (2010): *Specification ICC.1:2010 Image technology colour management — Architecture, profile format, and data structure,* ISO 15076-1:2010 / ICC.1:2010-12

ECO-DESIGN: FASHION AND TEXTILE INDUSTRY CHALLENGES AND EDUCATIONAL APPLICATIONS

Edit CSANÁK

Abstract: *Sustainability is an idea integrated into all creative industries, including the textile industry. The development of an eco-conscious approach has now become a cornerstone of modern textile and fashion design education. Eco-conscious fashion brands and "green collections" are born daily; analysts estimate that the trend towards environmentally conscious production of textiles and clothing will intensify in the context of increasingly apparent signs of climate change. Simultaneously, the interest of fashion-sensitive members of the self-conscious and environmentally conscious Y and Alpha generations will be increasingly focused on purposeful, eco-thematic training. Since the recent epidemic, it has been well known; there is great educational potential in on-line training on the theme of eco-design. However, it is not easy to develop up-to-date teaching material on a topic that has such a wide range of quality literature! This article presents a course module developed within a project funded by the European Union's Interreg Central Europe Programme, which deals with the textile and fashion design aspects of eco-design. This article intends to present the course content briefly.*

Keywords: *eco-design, Sustainable Fashion, fashion education, course module*

GOIN' GREEN

By "going green," we consider the process of changing thinking, attitudes, and lifestyles, and consumption habits, and its environmentally conscious approach. This responsible decision-making behavior advocates the long-term use, reuse, and recycling of products in all possible ways while reducing the impact of consumption on the environment. These conscious decisions will help protect the earth's renewable resources in the long run, focusing on their conservation rather than continuous exploitation. The green revolution is an environmentally conscious approach to living and thinking by making responsible choices to reduce the environment's imprint. It is considered a gradual process of changing the lifestyle by reusing and recycling products whenever possible and making choices that will help preserve the earth's non-renewable resources instead of destroying them. After three decades of work and struggle, the fashion industry's ethical and environmental movements have created a new segment in the fashion market: eco-design textiles and fashion products sustainable fashion segment. It also made new relations and interests. The purchasing decisions of self-conscious millennials, who grew up in the multicultural network of consumer society, are mostly driven by environmental awareness, in addition to quick conclusions.

The New Aage fashion consumer is interested in fashion only in it is environmentally, economically, and socially aware. For Generations Y and Alpha, who are committed to the Planet's future, it is natural that they are vividly attracted to making fashion sustainable. [1] [2]

SUSTAINABILITY IN THE TEXTILE AND FASHION INDUSTRIES

By sustainable fashion, we mean the processes by which fashion products are designed and manufactured responsibly, taking into account the environmental and social impacts of clothing and accessories. As a trend in sustainability in the textile industry, it aims to reduce the ecological footprint of industrial processes in the long term through and support environmental protection and social responsibility initiatives. As a movement and strategy, it promotes change at all levels of the industry. It aims to transform textile production and the fashion industry towards environmental integrity and social justice. The sustainability movement, which dated back to the late 1990s and became a global movement in 2013 due to known events, consciously and conceptually spreads the idea of sustainability through campaigns, professional events, and training. As a result, more and more people now agree that sustainable fashion is the only way for the fashion industry, so consumers pay more attention to shopping.

The project's training material highlights that the textile industry is one of the oldest sectors in consumer goods production, among the leading industries that impact the environment. This diverse and heterogeneous sector covers both natural and artificial raw materials, covering the entire production chain, transforming them into the most varied end-use goods - in cooperation with other actors in the economy. In terms of trade intensity, we are talking about the second-largest economic activity in the world. The cause of the "unsustainable state" of fashion is found in the constant market flow of new goods and globalized manufacturing processes. It has made it possible to produce clothes and clothing accessories at low prices that have created significant environmental threats over the past decade.

The paradigms shift, and moving towards sustainable fashion and raising awareness are renewable challenges for education. Active decision-making on social issues, meeting the criteria of transparency and sustainability, has recently become a next-generation fashion brand expectations. It is arguably essential in these processes that textile and fashion designers have a responsibility to incorporate the idea of sustainability into their production processes.

CIRCULAR ECONOMY IN THE TEXTILE AND FASHION INDUSTRY

In a holistic approach to the production of textile products, it is important to emphasize:

A.) The importance of production conditions and the environmental footprint of products on the environment throughout their life cycle;
B.) Effects can occur from fiber and filament production to dyeing or textile printing; the environmental footprint of finishing processes; energy used in production, waste;
C.) In addition to the economic and ecological aspects of the production of goods, social, cultural, and financial aspects.
D.) Since significant environmental impacts occur during use, raising awareness of the importance of taking responsibility is needed in all areas. All actors in the supply chain have a role in reducing the environmental footprint of textile products. A sustainable approach can be incorporated into critical stages of the product life cycle, all industry actors' daily routine. This

process begins with fashion and textile design education, as well as fashion product management education.

The circular economy is an economic system that aims to eliminate the continuous use of waste and resources to redefine growth, in contrast to the "take-make-waste" extractive industrial model. It also aims to keep products, equipment, and infrastructures in use for more extended periods, thereby improving their productivity by focusing on positive social benefits. Relying on renewable energies, the circular model builds economic, natural, and social capital over the linear one. Reducing the resources used helps to reduce pollution.

The concept bases on three principles: making waste and pollution predictable, keeping products and raw materials in long-term use, and continuously regenerating natural systems.

From linear to circular systems

The circular economy is a more sustainable system than the linear economy, in which all the "waste" has to become the "food" of another process. It features a system-oriented concept, durability and reusability, continuous renovation and recovery, and that maintains human needs and considerations. The textile industry is one of the sectors that has integrated the principle of the circular economy. (Fig. 1)

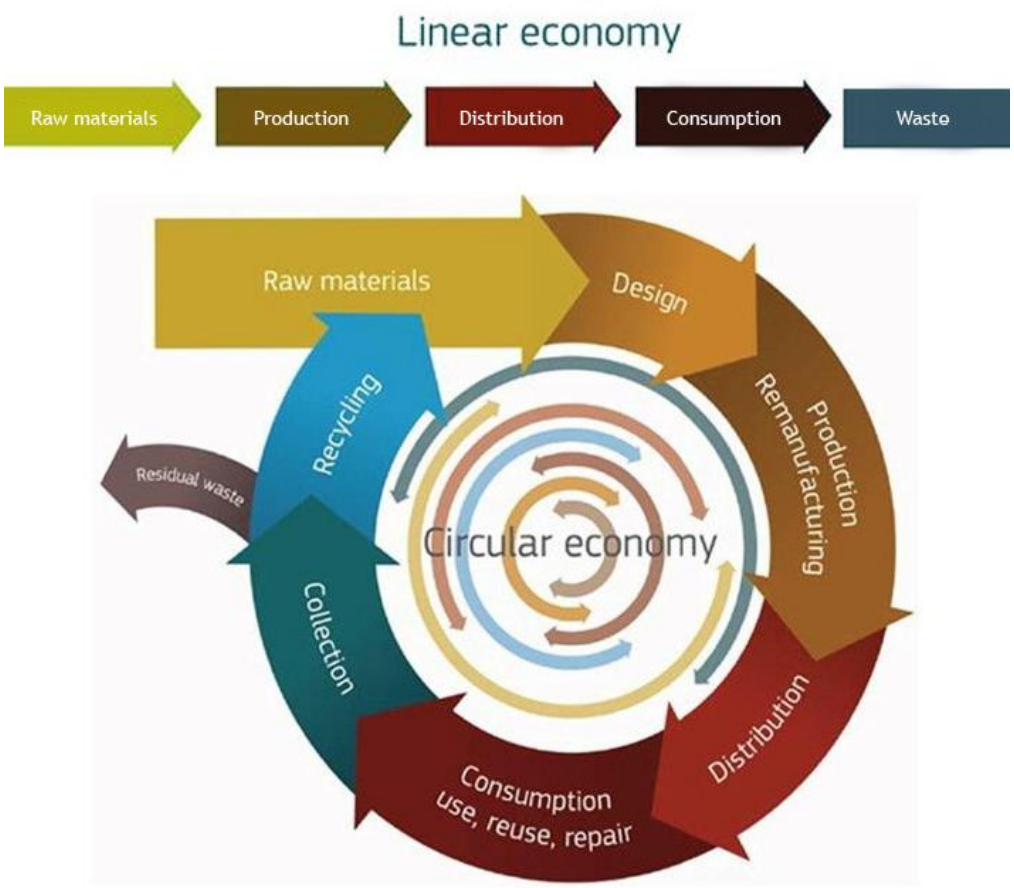

Figure 1: From linear to circular systems

In the textile and fashion industry, the circular economy means the continuous recycling of the fibers used to make garments and textiles, in response to the current linear model where raw materials are extracted, manufactured, purchased, used, and then discarded by consumers. With the circular economy model, the textile industry can be made a sustainable sector, with textile waste returning to the economy as much as possible.

The textile industry has a long way to go to achieve a sustainable future. The circular economy model's application can provide answers and solutions to the social and environmental issues arising from the current linear, "Fast Fashion" business model.

ECO-DESIGN

Ecological design, or popularly: eco-design, the science of eco-design methods that can be integrated into the sustainability trend, an environmentally conscious approach to product design; consideration of the environmental impact of the product throughout its whole life cycle. Ecodesign "applies to any form of design that minimizes the devastating effects on the environment by integrating itself into living processes." Eco-design has an impact on all areas of design and environment design: it affects the way and processes of designing and manufacturing clothing and accessories, but also the creation of household appliances, furniture, and toys. It is also present in architecture, lighting and energy design, and transportation.

Environmentally conscious textile and fashion design

The natural world has always inspired designers. As the fashion industry has underexploited natural resources and wildlife, fashion's relationship with nature has deteriorated over the past few hundred years. There is a need to change attitudes, practices, and innervations, which means rejecting the exploitation of wildlife and natural resources for dressing purposes. New, less destructive, healthy, and sustainable communication with the world is achieved by maintaining "well-dressed" conditions appropriate to environmental and climatic conditions, keeping pace with technological development and civilization's expectations, while consistently reflecting the cultural, social, and - and social affiliation and individuality.

Eco-fashion is an environmentally conscious approach to the design and manufacture of clothing and accessories, taking into account, in addition to the above, environmental considerations, the health of consumers, and the working conditions of workers. Eco-fashion products are made: 1. By using organic raw materials grown without pesticides; 2. By avoiding fabrics treated with harmful chemicals and bleaches; 3. Often from recycled and reused textiles or recycled fibers; 4. Made to last so that people can keep them for longer; 5. Made under the conditions of "fair trade."

AREAS OF ECO-DESIGN ACTION IN THE TEXTILE INDUSTRY

The circular economic model's fundamental goal is to improve the quality of life by maximizing ecosystems' potential in the long run and using the right technologies. The new paradigm requires us to look at routine processes differently. For example, the textile and fashion industries use large amounts of water and energy; the two are highly worrying resources worldwide. The production and consumption of both fashion and textiles are a significant source of pollution. The eco-conscious design offers several solutions to solve these.

Application of the "cradle to cradle" principle

The Cradle to Cradle (C2C) principle is a biomimetic method of designing products and systems. A system that models industrial processes in the light of natural processes has also been applied in the fashion industry. The flow of fashion products in a closed system, i.e., based on the C2C principle, increases the fashion industry's sustainability.

The use of environmentally friendly, easily recyclable raw materials, efficient and energy-saving production processes and production methods must be considered in the design and production to consistent application of the principle. To create value, the designer must pay attention to economic and environmental, and social aspects. Interactive approaches and close collaboration with supply chain actors are ways to achieve greater sustainability and significant benefits. [3]

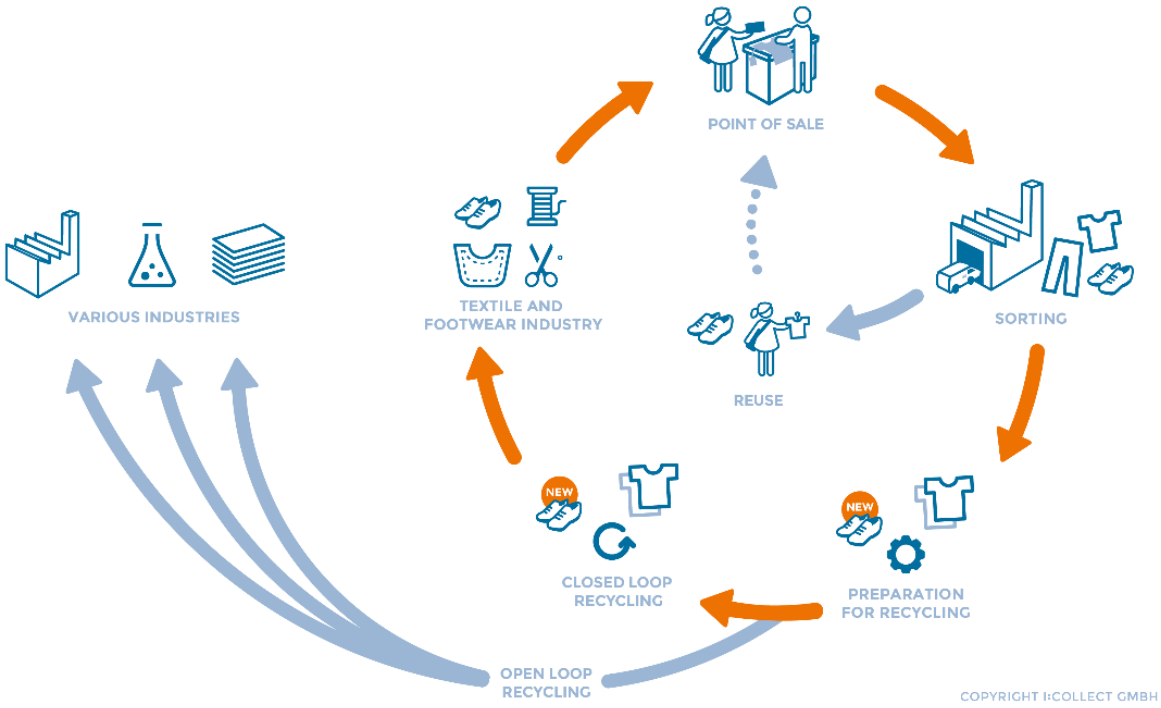

Figure 2: Flowchart of the closed and open system of the clothing supply chain (Source: ico-spirit.com)

Waste management solutions

There is a lot we can do to protect the environment through a **redesign**. The first recycling concepts were born in the hippie era of the 60s. The use of "treasures" found in second-hand stores to redesign, recycle, and renovate existing, bored, discarded, and useless items still inspire many designers.

Resale and clothing rental services have become an increasing trend in the fashion market to extend clothing life. Many clothing brands have already integrated the resale and used clothing sales business model into their profiles. "Clothing as a service" also seems to be becoming a basic business model in the fashion market.

The **clothing repair** culture, which had been lost for decades as an almost extinct activity, was back in vogue. As part of the slow fashion trend, many companies offer repair services to their customers to help extend the life cycle of the clothes they purchase in their chain. (Fig.3)

Recycling is the operation or process of converting waste into recyclable material. Fibers of various origins in clothing (natural, artificial, including many different types) are challenging for recycling.


Figure 3: Illustrations from the tutorial

ECO-APPROACH TO FASHION-MAKING

Eco-fashion is a complex and multifaceted relationship with the environment. Many believe it was sought first time after in the hippie style of the 1960s. The seeds of eco-fashion in the modern sense were taken by the profession in the early 1990s when environmentally friendly fabrics increased. From the beginning of human civilization, the use of natural (animal, plant) raw materials was evident, as was the fact that humans made as much clothing as they used. With the introduction of synthetic fibers since the middle of the twentieth century, when the textile and clothing industry met mass demand with relatively cheap quality, the situation has changed. It is now clear that creation without knowing the ultimate purpose is a waste of time, energy, and resources! Choosing the right material and technology is the key to the future sustainability of the fashion industry.

Figure 4: Illustrations from the tutorial

Environmentally friendly raw materials and production technologies

Complex and diverse scientific models are available and used to assess the environmental impact and ecological sustainability of different textile fibers. Factors influencing tissue sustainability:

- The ability and source of fiber renewal
- The process of processing the crude fiber
- Effects of fiber preparation and dyeing
- Energy used in the production process

Also: the working conditions of the people producing the materials, the total environmental footprint of the material, the transport conditions, the handling and washing of the product, and; *What happens to the product at the end of its life?*

Conscious, sustainable, and transparent production processes

Widespread environmental awareness has made textile, and fashion companies realize that reputation, transparency, and environmentally friendly manufacturing are the new "state-of-art." Key players in the fashion industry are collaborating to develop industry-wide sustainable technology solutions and processes. The global introduction of extended producer responsibility requires fashion companies to reduce their waste and pay their employees a fair and equitable living wage. Transparency in the clothing supply chain is now the foundation of a fashion company after most fashion companies have acknowledged that a reputation costs more than an investment. Transparency of textile supply chains is a universal goal, in which training, networking, and associations have a crucial role to play.

Introduction to organizations, projects, cooperation, and good practices play an essential role in eco-design education.[1]

[1] The training path concludes with a presentation of organizations, inspirational collaborations, student work, valuable initiatives, and a list of well-known international bibliographies relevant to the field.

SUMMARY

The sustainability of fashion, as a trend, seems to be strengthening today in the context of climate change. The interest of members of the self-conscious and environmentally conscious millennial generation, raised in consumer culture and receptive to textiles, clothing, and design, is focused on market-oriented, concept-oriented, consciously structured, exciting, and competitive eco-thematic training. Well-structured eco-design themes cover a wide range of topics that will enable a skilled generation of young professionals to make fashion truly sustainable in a real sense. This paper summarized the content of such a training material developed within the ENTeR project framework (CE 1136), implemented with the support of the European Union under the Interreg Central Europe Program.[2]

The training path has also been introduced in several Hungarian and international conferences, fashion forums,[3] and an article on-demand. It has also been published in Hungarian translation about the training path material. [1] All this justifies the increased interest in eco-design topics in textile and fashion education. This article presented such an e-training, pointing out the issues that need to be taught in eco-design education.

REFERENCES

[1] E. Csanák, “Ökodizájn a textil- és ruhaiparban,” *MAGYAR TEXTILTECHNIKA (ON-LINE 2008-) 2060-453X*, vol. 3, pp. 26-29., 2020.

[2] E. Csanák, "Sustainable Fashion: Limiting a Singularity-Advanced Glossary to an Article," *International Journal of Fashion Technology & Textile Engineering (Open Access)*, vol. 1, no. 1, pp. Pg 1-5., 2018.

[3] E. Csanák, "ECO-FRIENDLY CONCEPTS AND ETHICAL MOVEMENTS IN THE FASHION INDUSTRY," in *University of Zagreb*, Zagreb, 2014.

[4] E. Csanák, "Öko-design tematikák a divattermék menedzsment, a ruházati formatervezés és textiltervezés oktatásban," in *Tudományos-, Műszaki és Művészeti Közlemények*, Budapest, Óbudai Egyetem Rejtő Sándor Könnyűipari és Környezetmérnöki Kar, 2019, pp. pp. 78-89..

[2] You can find information about the project at the following link: https://www.innovatext.hu/hu/innovacio/nemzetkozi-projektek

[3] Donghua University (DHU) THE SUSTAINABLE FASHION FORUM - 8-9 December 2020

OPTIMIZATION OF LASER CUTTING OF REINFORCED PVC SHEET

Tamás CSISZÉR, Gabriella OROSZLÁNY, Edina KULCSÁR, Zsolt BORKA, Eszter KORMÁNY

***Abstract**: Composite sheets are widely used. These sheets are usually composites, consisting of a polymer matrix and fiber materials. Since there is a need for sheets in different sizes, they must be cut in parts. Several cutting technologies are used for this purpose, e.g., application of special knives, scissors, or water-jet. Besides their well-known benefits, there are some disadvantages, partly due to the direct connection between the tool and the material. To reduce, the application of laser beam cutting technology has expanded in the last decades. The purpose of our research was to test the application of a laser beam in cutting reinforced PVC sheet to find the optimal technology parameters. We found that a CO2 laser machine can cut PVC-PA composite sheets with acceptable edge quality. Optimal parameter setting is V = 100 mm/s cutting velocity and P = 30 W laser power. The experiments could not prove the correlation among line energy, edge quality, and area of HAZ. V has a significant effect on tensile strength with 20 and 30 mm/s. The maximum tensile strength is 868 N for warp cutting direction, which was produced by V = 25 mm/s.*

***Keywords**: PVC, reinforced polymer, laser cutting*

INTRODUCTION AND LITERATURE

The laser beam application in cutting polymers is a popular technology because it offers excellent potential to process a wide variety of materials. [1] The surface quality aspects of laser cutting were investigated in the case of some polymeric and composite materials as polycarbonate (PC), polymethylmethacrylate (PMMA) (acrylic), polypropylene (PP), and thermoset plastics. Several levels of power, cutting velocity, and pressure settings were used during the process. At the preliminary tests, the following process parameters were used: the laser power and the cutting velocity were varied from 280 to 900 W, and 250–4000 mm/min, the thickness of the selected plates varied from 2 to 8mm, and the range of gas pressure was 0.5–4 bar. The processing parameters used for the CO_2 laser cutting of PMMA and PC were as follows: laser power and the cutting velocity were varied from 250 to 650 W and 250–3500 mm/min. The thickness of the selected plates for the PMMA and PC was 6 and 3 mm. The pressure of the gas for CO_2 laser cutting PMMA and PC were 0.5 and 4 bar. The results showed that the heat-affected zone (HAZ) increases with laser power and decreases with the cutting velocity. The laser cutting workability of the polymers/composites: PMMA very high, PC high, PP high and medium, and thermosets plastics lower. [2]

CO_2 laser cutting application was also investigated to polyethylene (PE), polypropylene (PP), polycarbonate (PC) in different thicknesses ranging from 2 to 10 mm. Besides the parameters mentioned above, the values of kerf widths on top (Lsup) and bottom (Linf) thicknesses, the melted transverse area, the melted volume per unit time, and surface roughness values (Ra) on cut edges were also measured during the process. According to the results, not always higher

cutting speeds are indicative of greater process efficiency. The laser cutting workability of the three polymers is as follows: PC high, PP medium-high, and PE lower. [3]

The laser process was also used for the cutting of medium-density fibreboard (MDF). The CO_2 laser was used during the operation in continuous wave and pulse mode also to compare the cut quality results. In constant wave, results showed that the average kerf width obtained for MDF reduced with increasing cutting speed for most material thickness. The experimental results also showed that the greater the cutting speed, the less time there was for heat to diffuse sideways through the cut surfaces and the narrower the HAZ. In the case of pulse mode, the difference in Ra and the kerf width was slight. [4]

In another application of a 60W CO_2 laser on polycarbonate sheet with a thickness of 3.2 mm they concluded that by decreasing the laser focal plane position and laser power, the bottom kerf width was reduced, and the bottom kerf decreases if the cutting speed increases. The cutting quality is better if the laser spot point locating in the depth of the workpiece. The optimum process parameters were as follows: cutting speed 16 mm/s, laser power 40W, focal plane position 1.8 mm. [5]

Carbon fiber reinforced plastics (CFRP) show a high potential for use. Laser cutting of the CFRP was examined in more aspects. The applicability of the laser remote cutting process and the gas-assisted laser cutting of CFRP were analyzed. Based on the experiments' results, both are suitable to cut the CFRP material [6]. In another investigation, a systematic analysis of the hazardous substances emitted during laser cutting of CFRP with thermoplastic and the thermosetting matrix was demonstrated. The result of the mass-spectrometric analysis was that the emissions of dangerous substances are significant. However, it is possible to minimize these hazardous substances in the workplace, not to exceed the thresholds. [7] The quality of the cut surface and the material properties were influenced using laser cutting. The cutting process is improved, and fewer errors occur if adding light-absorbing soot particles to the matrix's resin. [8]

The experiments introduced above did not apply CO_2 laser to process PVC sheet, so its optimal values of technology parameters are not identified yet. We prepared experiments to identify applicable technology window and optimal values of power and velocity to fill this gap.

SPECIFICATION OF MATERIALS AND EQUIPMENT

Test material is produced by Tuplex. Its most important features are the followings:

- Excellently compatible with UV curable digital printers;
- Perfect printing impression with stable ink absorption and low ink consumption;
- Good physical strength in longitude and latitude;
- High glossy and smooth surface;
- Matte back prevents stickiness.

The technical properties are presented in Table 1.

Table 1: Technical properties of test material

Product name	Tuprint Frontlit Banner, C1010-450
Chemical Compound	Polyvinyl-chloride (PVC) and Polyester (PE)
Base Fabric	1000D*1000D polyester yarn
Area Density	510 g/m^2
Fabric Thickness	0,376 mm
Warp density	63 pcs/100 mm
Weft density	72 pcs/100 mm

The material was cut by an ALFA LCE – 2 CO_2 Laser machine. Images were created by JINGOU Portable USB Digital Microscope and were assessed by ImageJ software.

EXPERIMENTS

Preparatory Experiments

The purpose of the preparatory experiments was to identify the technology window provides acceptable edge quality. Parameter settings of preparatory experiments are shown in Table 2.

Table 2: Parameter settings of preparatory experiments

Power of laser beam (varied)	10 – 60 W (with 10 W step)
Cutting velocity (varied)	10 – 100 mm/s (with 10 mm/s step)
Focus distance (constant)	58 mm
Cutting length (constant)	850 mm
Mode (constant)	Pulse, 20 kHz
Direction of irradiation (constant)	Back non-printed side of sheet
Direction of cutting (constant)	Weft

One 30 cm long cut was made for every combination of varied parameters (demonstrated in Figure 1). From each cut 3, 10 mm length section was selected for the assessment of edge quality.

Figure 1: Some of the cuts on the back side of PVC sheet

The area of Heat Affected Zone (HAZ) was measured by ImageJ software.

The values of the area of HAZ for different laser parameters are shown in Table 3 and Fig. 2.

Table 3: Area of HAZ measured by ImageJ software with settings I

Area of HAZ [mm^2]		Laser power [W]				
		20	30	40	50	60
Cutting velocity [mm/s]	10	5,493E-01	6,117E-01	4,833E-01	6,080E-01	5,927E-01
	20	3,223E-01	3,603E-01	3,920E-01	3,470E-01	2,673E-01
	30	4,217E-01	3,893E-01	3,787E-01	3,637E-01	2,937E-01
	40	8,543E-01	3,863E-01	3,783E-01	3,883E-01	3,317E-01
	50	8,617E-01	3,900E-01	3,693E-01	3,780E-01	3,483E-01
	60	6,433E-01	2,087E-01	2,547E-01	3,217E-01	2,183E-01
	70	7,550E-01	3,300E-01	3,923E-01	2,507E-01	2,760E-01
	80	1,115E+00	5,510E-01	4,647E-01	4,567E-01	3,737E-01
	90	1,012E+00	4,313E-01	4,873E-01	4,827E-01	4,233E-01
	100	8,600E-01	1,823E-01	1,940E-01	2,550E-01	2,747E-01

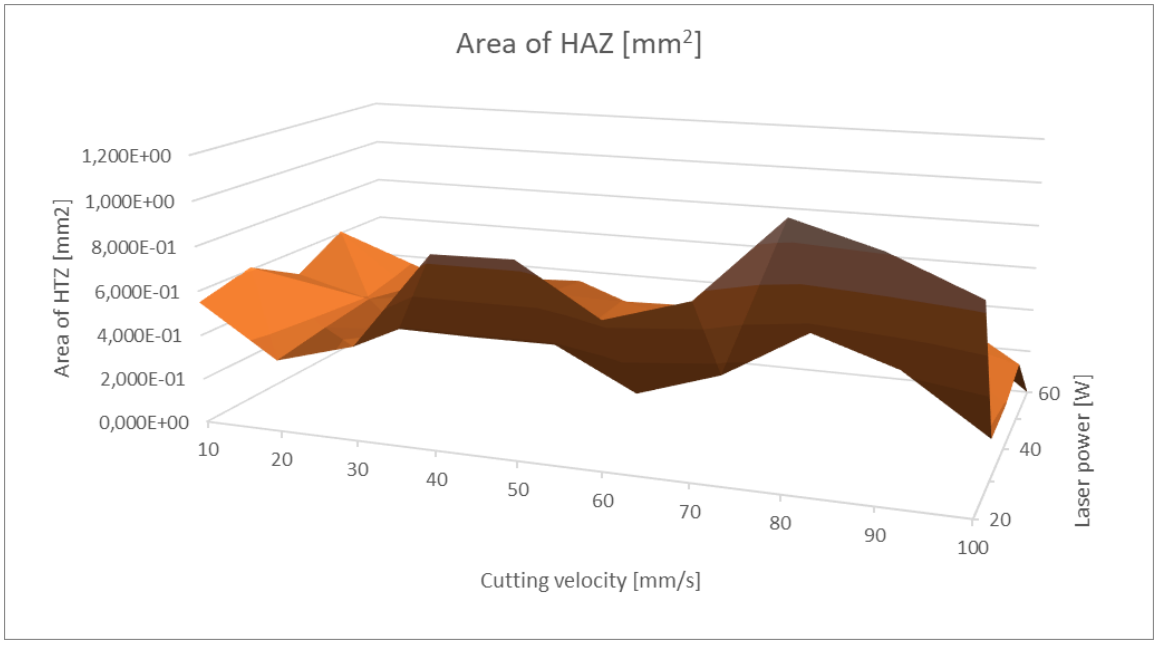

Figure 2: Area of HAZ measured by ImageJ software with settings I

Edge qualities of the selected 3 sections were analyzed by visual inspection by two inspectors too. If HAZ could be seen by eyes without a microscope, the result of qualification was 1. Since two inspectors checked 3 sections, the maximum level of negative qualification for each specimen is 6.

Based on the inspection, the following conclusions could be drawn:

- With 10 W laser power, the sheet could not be cut, which means that more than 10 W is needed to cut the material tested.
- At 10, 20, and 30 mm/s velocity the area of HAZ could not be recognized by eyes.
- At 20 W laser power, HAZ could be measured by microscope in case of every velocity, but could not be detected by eyes below 30 mm/s. The area of HAZ was bigger than that of all of the other values of power above 30 mm/s. The detected area was the yellow zone of the sheet, probably caused by condensed gases of ingredients.
- Another HAZ peak was detected by ImageJ measurement at 10 mm/s velocity. The area of HAZ was increased by the increase of power. However, this HAZ could not be recognized by visual inspectors. This might be caused by the continuously changing grey colour of this zone, which made it difficult to detect by eyes, but it could easily be measured by microscope.
- From the processing point of view, we need high velocity for small cycle time and low power for cost-effectiveness, resulting in acceptable edge quality, so if we assume that the PVC sheet was homogeneous, the optimal combination of parameters is V = 100 mm/s and P = 30 W.

To identify the correlation between laser settings and assessment results, we compared the values of line energy, visual qualification, and area of HAZ [see in Figure 3, Figure 4, and Figure 5. Line Energy is defined as the ratio of laser power [P] to cutting velocity [V] [8].

$$E = \frac{P}{V}\left[\frac{J}{mm}\right] \quad (1)$$

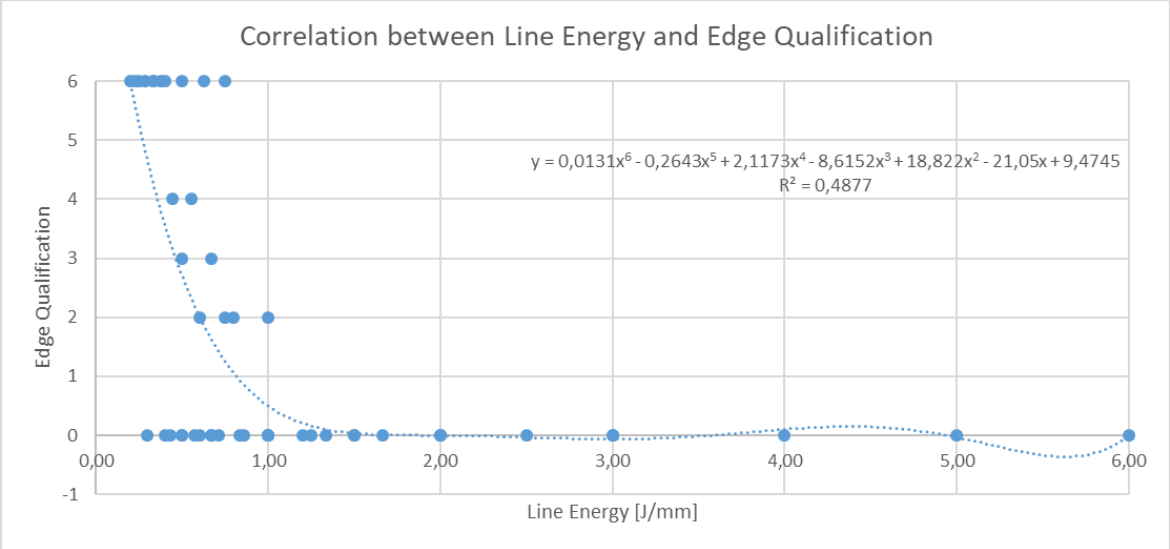

Figure 3: Correlation between Line Energy and Edge Qualification

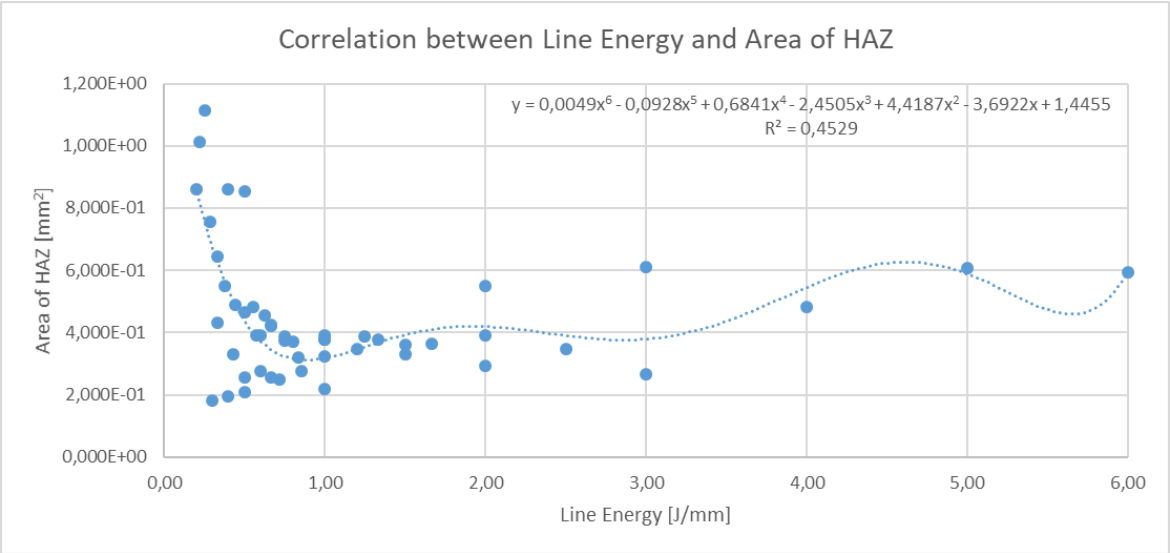

Figure 4: Correlation between Line Energy and Area of HAZ

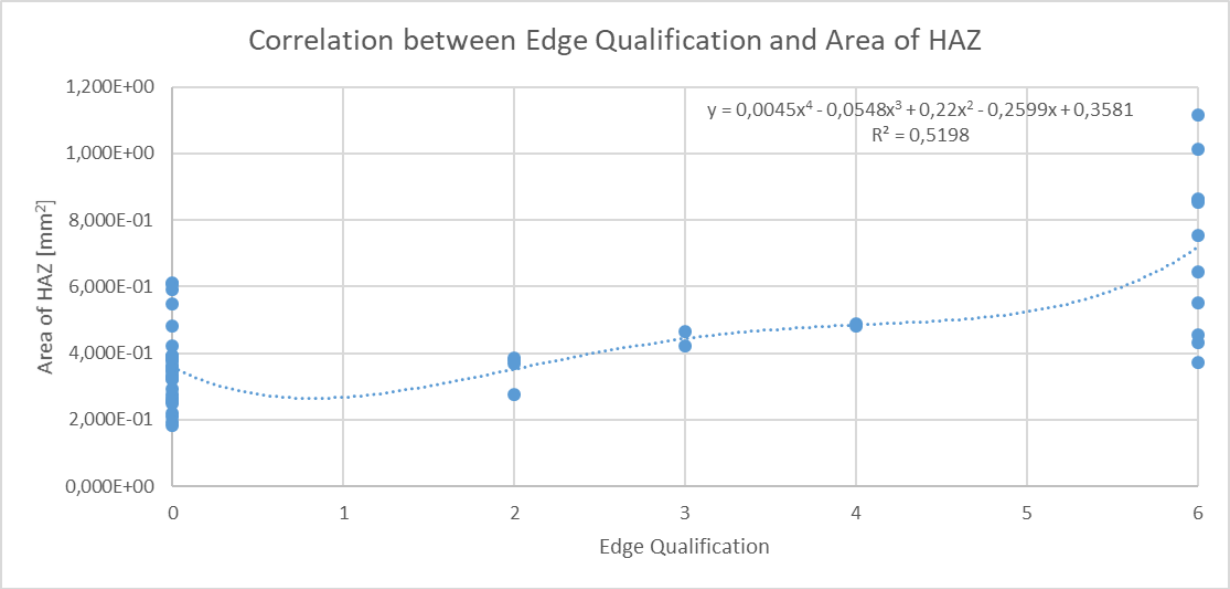

Figure 5: Correlation between Edge Qualification and Area of HAZ

Results show that there are not correlations among these factors, which means there must be other factors that influence edge qualification. Besides, there is no correlation between the Area of HAZ and visual qualification.

Assessment of HAZ for Negatively Qualified Specimens

We measured HAZ with different ImageJ settings too [see in Figure 6] to check whether the correlation between factors could be identified if we take only unaccepted specimens into consideration. The value of brightness was set to harmonize with the visual detectability, which means that those specimens that were accepted by visual instructors have zero HAZ.

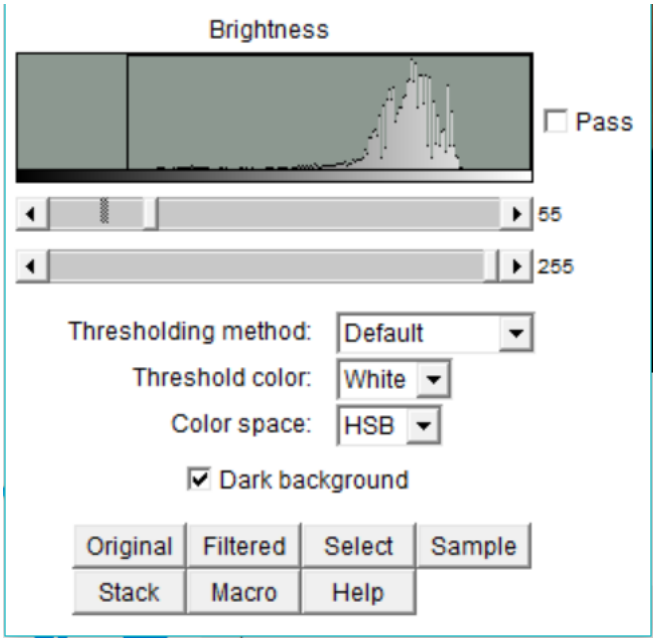

Figure 6: Settings II of threshold color in ImageJ for the measurement of the area of HAZ

The areas of HAZ measured by new settings for previously unaccepted specimens by visual inspection are presented in Table 4 and Figure 7.

Table 4: Area of HAZ measured by ImageJ software with settings II

Area of HAZ [mm^2]		**Laser power [W]**				
		20	**30**	**40**	**50**	**60**
Cutting velocity [mm/s]	**40**	1,933E-02	1,500E-02	N/A	N/A	N/A
	50	1,367E-02	N/A	1,788E-03	6,000E-03	N/A
	60	4,247E-03	N/A	N/A	N/A	N/A
	70	2,816E-03	N/A	N/A	N/A	N/A
	80	5,526E-03	6,000E-03	5,493E-03	6,370E-03	2,221E-03
	90	7,411E-03	1,667E-03	4,347E-04	1,000E-02	5,339E-04
	100	7,124E-04	N/A	N/A	N/A	1,955E-04

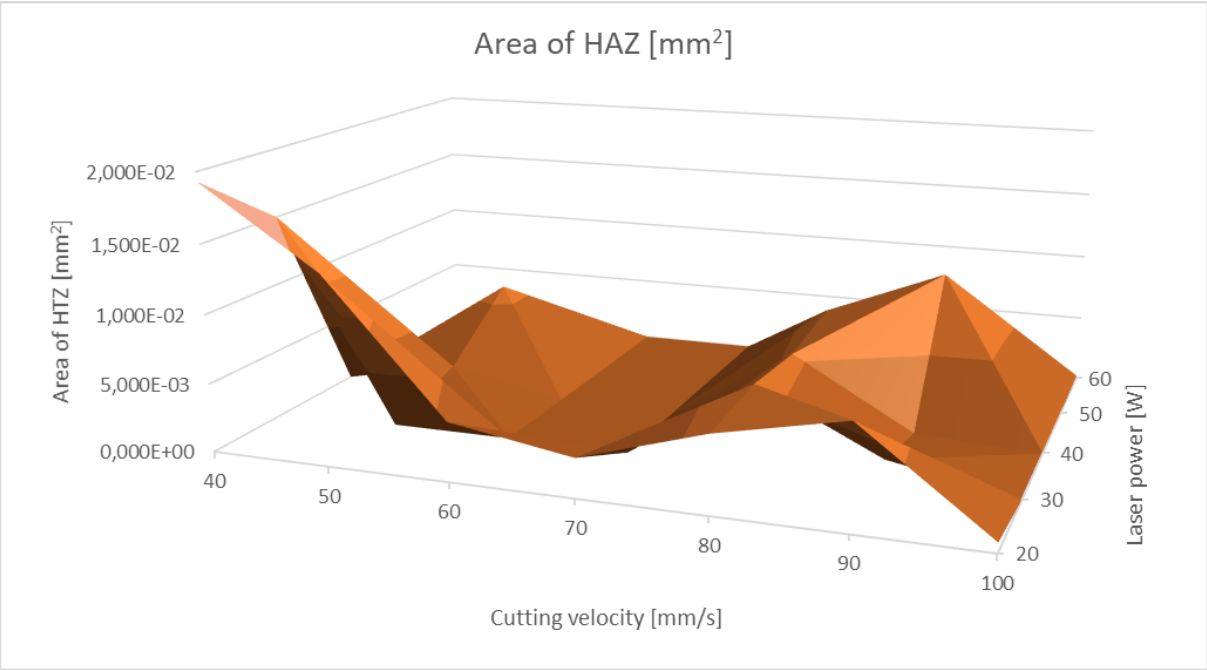

Figure 7: Area of HAZ of visually unaccepted specimens, measured by ImageJ setting II

We can conclude that a strong correlation could not be found between any of the factors.

Assessment of Mechanical Properties

The purpose of the next experiment was to assess the connection between cutting technology parameters and tensile strength expressed in maximum force [F_{max}]. We applied both thermal and mechanical effects. The list of independent or input variables is specified in Table 5. The list of dependent or output parameters is specified in Table 6.

Table 5: Input parameters of cutting experiment

Power of laser beam (varied)	40, 45, 50, 55, 60 W
Cutting velocity (varied)	20, 25 and 30 mm/s.
Cutting method (varied)	A laser beam, knife, scissors
The direction of cutting (varied)	Weft and warp

Table 6: Output parameters of cutting experiment

Maximum tensile force [N]
Elongation [%]

The design of the experiment is specified in Table 7. The number of specimens is 5 for every combination.

Table 7: Design of cutting experiment

ID.	Laser power [W]	Cutting velocity [mm/s]	Cutting method	Direction of cutting
1	40	20	laser	weft
2	40	20	laser	warp
3	40	25	laser	weft
4	40	25	laser	warp
5	40	30	laser	weft
6	40	30	laser	warp
7	45	20	laser	weft
8	45	20	laser	warp
9	45	25	laser	weft
10	45	25	laser	warp
11	45	30	laser	weft
12	45	30	laser	warp
13	50	20	laser	Weft
14	50	20	laser	Warp
15	50	25	laser	Weft
16	50	25	laser	Warp
17	50	30	laser	Weft
18	50	30	laser	Warp
19	55	20	laser	Weft
20	55	20	laser	Warp
21	55	25	laser	Weft
22	55	25	laser	Warp
23	55	30	laser	Weft
24	55	30	laser	Warp
25	60	20	laser	Weft
26	60	20	laser	Warp
27	60	25	laser	Weft
28	60	25	laser	Warp
29	60	30	laser	Weft
30	60	30	laser	Warp
31	Manual	Manual	scissors	Warp
32	Manual	Manual	knife	Warp
33	Manual	Manual	scissors	Weft
34	Manual	Manual	knife	Weft

Comparing thermal and mechanical processing, results do not prove that there is a significant difference between their effects on tensile strength. Results show that only cutting velocity has a significant effect on tensile strength at 0,05 significance level (Figure 8).

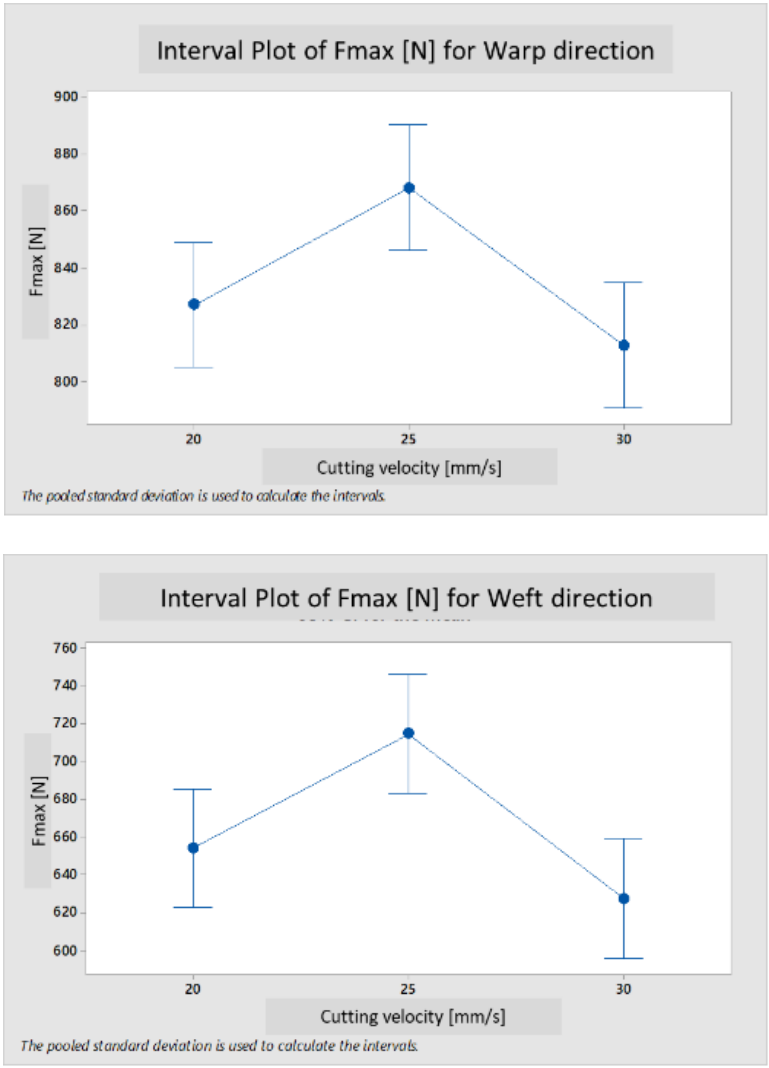

Figure 8: Results of One-way ANOVA: a) cutting in the warp direction (P-Value is 0,002); b) cutting in weft direction (P-Value is 0,001)

The optimal value of cutting velocity is 25 mm/s for both cutting directions. The maximum value of average tensile strengths is 868 N for warp direction and 714 N for weft direction (Figure 9 and Figure 10). For weft direction, cuttings by all the velocities result in higher tensile strength than that of mechanical cutting (Figure 9). For warp direction, the cuttings with knife and scissors result in higher tensile strength than that of laser beam cutting at 20 and 30 mm/s, while there seems not to be a significant difference between the result of mechanical cuttings and thermal cutting at 25 mm/s velocity (Figure 10). Weaker strength can be caused by the bigger HAZ, but this could not be detected. Another reason can be the heterogeneity of material.

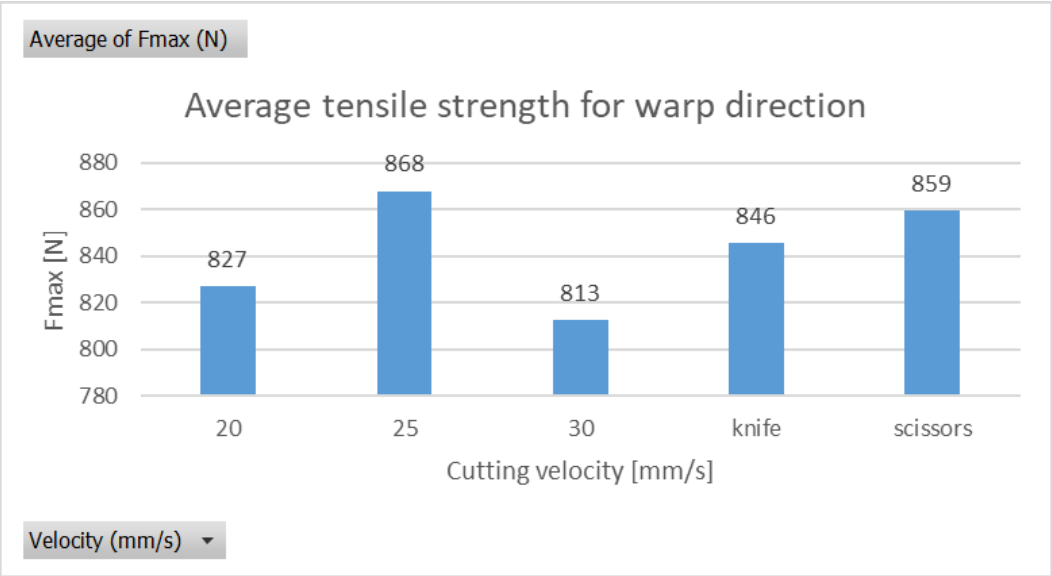

Figure 9: Effect of the velocity of cutting [mm/s] in warp direction on tensile strength (Fmax [N])

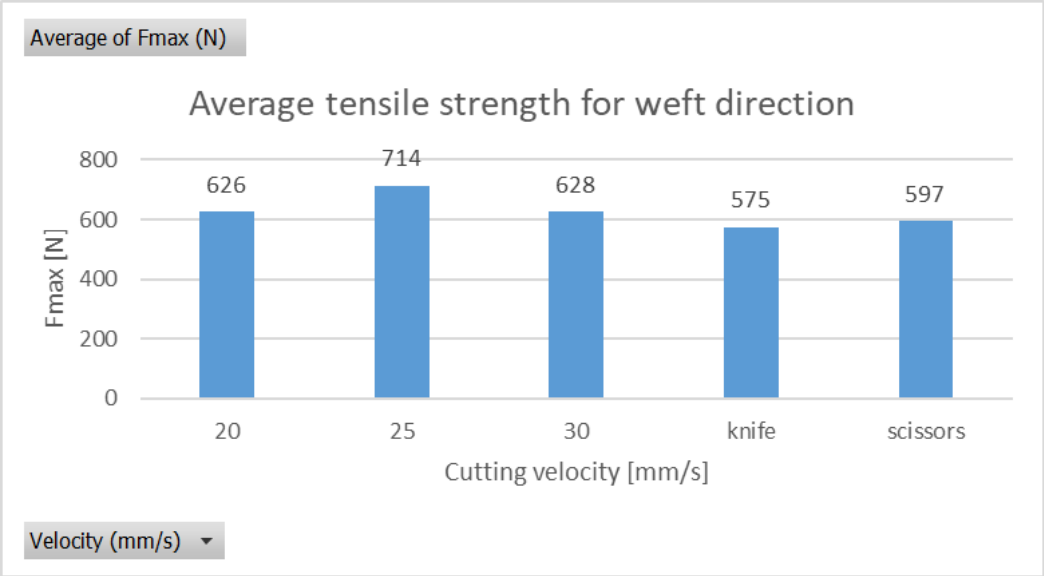

Figure 10: Effect of the velocity of cutting [mm/s] in weft direction on tensile strength (Fmax [N])

CONCLUSIONS

PVC-PA composite sheets can be cut by a CO_2 laser machine with acceptable edge quality. Optimal parameter setting is V = 100 mm/s cutting velocity and P = 30 W laser power. The correlation among line energy, edge quality, and area of HAZ could not be proved by the experiments. V has a significant effect on tensile strength with 20 and 30 mm/s. The maximum tensile strength is 868 N for warp cutting direction, which was produced by V = 25 mm/s. The effect of laser power on tensile strength could not be proved between 40 and 60 W.

REFERENCES

[1] http://alfalaser.hu/wp-content/uploads/2017/01/ALFA-LCE-2-mont%C3%A1zs.jpg

[2] Goeke, A., Emmelmann, C.: Influence of laser cutting parameters on CFRP part quality. Physics Procedia (2010), pp. 253-258

[3] Davim, J. P., Barricas, N., Conceicao, M., Oliveira, C.: Some experimental studies on CO_2 laser cutting quality of polymeric materials. Journal of materials processing technology (2008), pp. 99-104

[4] Caiazzo, F., Curcio, F., Daurelio, G., Minutolo, F. M. C.: Laser cutting of different polymeric plastics (PE, PP and PC) by a CO_2 laser beam. Journal of Materials Processing Technology (2005), pp. 279-285

[5] Lum, K. C. P., Ng, S. L., Black, I.: CO_2 laser cutting of MDF: 1. Determination of process parameter settings. Optics & laser technology (2000), pp. 67-76

[6] Spena, R. P. CO_2 Laser Cutting of Hot Stamping Boron Steel Sheets. Metals (2017), pp 1-18

[7] Klotzbach, A., Hauser, M., Beyer, E.: Laser cutting of carbon fiber reinforced polymers using highly brilliant laser beam sources. Physics procedia 12 (2011): pp. 572-577

[8] Walter, J. et al.: Laser cutting of carbon fiber reinforced plastics–investigation of hazardous process emissions. Physics Procedia 56 (2014), pp. 1153-1164

DETERMINATION OF MEASUREMENT UNCERTAINTY IN A COMPLEX TESTING PROCESS FOR TEXTILE TESTS

Tibor GREGÁSZ, Veronika PÁL, Vera GÖNDÖR

***Abstract**: All standards dealing with colorfastness testing of textiles avoid the issue of measurement uncertainty. However, this does not exempt accredited testing laboratories from the obligation to assess the factors of measurement uncertainty required by ISO/IEC 17025:2017. This is where the abstract text comes. This is a sample. This paper identifies and classifies the uncertainty components of the most frequent textile colorfastness testing procedures. As the test method comprises chemical, mechanical, and visual elements, the results are subject to complex uncertainty factors. Using experimental data, measurement results, and their statistical evaluation, we inquire into factors that allow defining a numerical uncertainty value for the respective test method. The result obtained allows continuous improvement of the procedure.*

***Keywords**: measurement uncertainty, colour fastness testing, visual assessment, R&R*

INTRODUCTION

This research addresses the current and complex problem of determining measurement uncertainty in an accredited and designated textile laboratory. The research focuses on colour fastness testing, which has several different subtypes. As the subjective factor is significant in each test method, the measurement uncertainty is also difficult to quantify. For this reason, it has not yet been accurately defined and evaluated in similar laboratories. The ISO 17025:2017 standard places greater emphasis on the assessment of measurement uncertainty, the determination of its components, their evaluation, and, in the case of a complex method, its estimation as a general requirement of testing laboratories. [1] Currently, there is no method to adopt for this type of test method to provide measurement uncertainty. Our research will help the laboratory meet the requirements of laboratory accreditation, and for this test type, we will need to define sources of measurement uncertainty and quantify it using the appropriate analytical method. The purpose of the research is to support the textile testing laboratory in this topic by systematizing and evaluating the measurement uncertainty factors for the most common colour fastness tests. Furthermore, experimental quantification of the variance components of a particular test method will give us a specific uncertainty value.

PRINCIPLE AND STRUCTURE OF COLOR FASTNESS TEST METHODS

Throughout this research, we analyzed the six colorfastness tests most in demand: which are namely to water, perspiration, rubbing, baby saliva and perspiration, washing, and dry cleaning. The principle of the above tests is to subject the dyes or prints on fabrics or fibers to various chemical and/or mechanical stress simulations. Consequently, we can obtain two kinds of results in the so-compared to grayscales:

- classification of the specimen's change of color due to wet and chemically active medium,
- the intensity of the staining on the white adjacent fabrics attached to the specimen. (The latter is generally expected to be more relevant.)

With the use of the greyscale, the darkness of the adjacent fabrics is quantified by one of the values 1/2 on a scale of 5. Here, 1 is the worst (meaning the greatest darkness), and 5 is the best (meaning remaining white/unchanged), but half grades can be given. [2] [3] [4]

Figure 1: Part of the grayscale (grades 1-3) to assess staining (top) and colour change (bottom)

The steps of the test methods in question are illustrated by the following figure. The model of action used in each study depends on the type of exercise tested. For each specimen, either a standard single or multifibre (a special weave of six different components) adjacent fabric is attached, as required by the standard. For practical reasons, the former was used in the experiments of this study. The sample fixed between the adjacent fabrics is called a composite specimen.

The most sensitive part of colour fastness tests - thus, the most regulated part by standards - is the visual evaluation of pre-treated composite specimens. This is done under strict conditions in a 6500K colour temperature, special grey cabinet (colour viewing booth) with D65 sunlight to provide the observer with a neutral ("inert"), reflex-free, and always the same angle of sight. [2] [3]

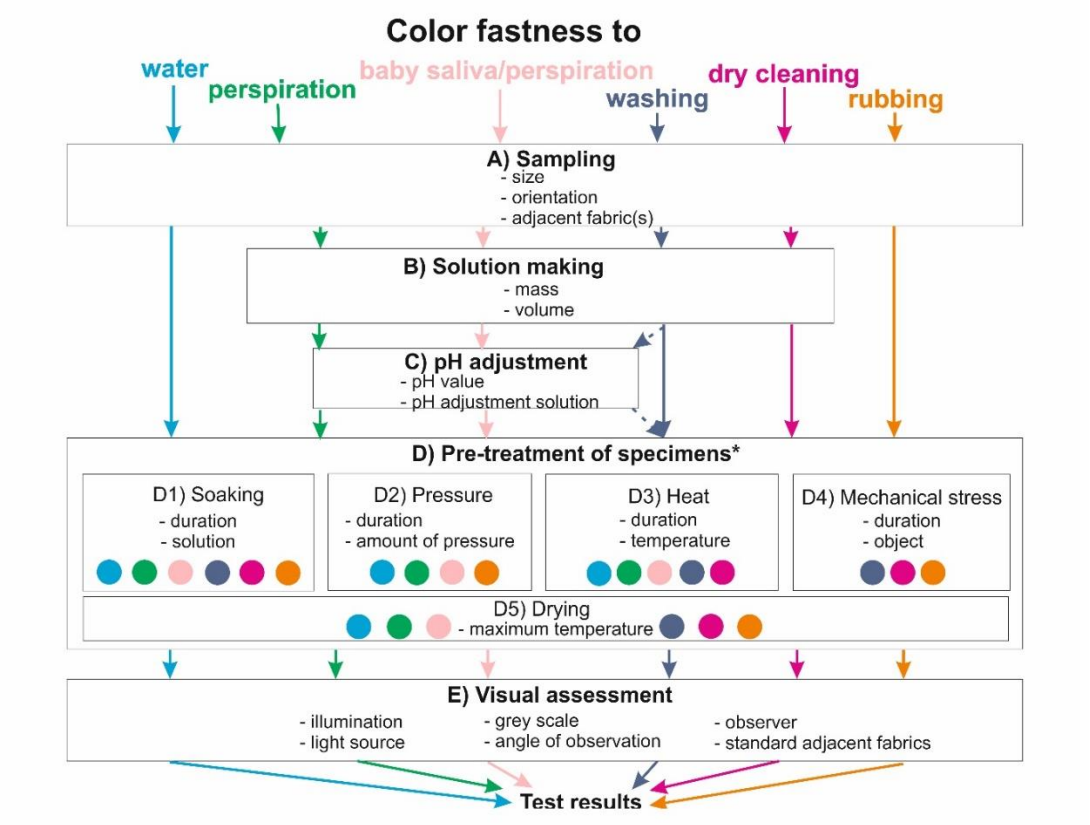

Figure 2: Process of six colour fastness tests and the most important parameters

INTERPRETATION OF MEASUREMENT UNCERTAINTY

It is acceptable even for laymen that a measurement result, due to its many influencing factors, can never be completely identical and will deviate from its true value; that is, it is loaded with an error. The phenomenon and this property of the measurement procedures are, according to the most commonly used wording: "parameter, associated with the result of a measurement that characterizes the dispersion of the values that could reasonably be attributed to the measurand." It can be given by the variation characteristic calculated from the measurement results (Type A determination) or by other scientifically valid information (Type B determination). [6] [7] [8]

It can be expressed as an accurate numerical value using various statistical features; in a direct, "one-dimensional" measurement where we want a relatively easy-to-measure parameter (such as weight measurement), the results obtained are called repeatability standard deviation can also be given as "s." This can be considered the same as the "standard uncertainty," which is called "u" (u - uncertainty). Another solution is the so-called "extended uncertainty" U, for which

$$U = k \cdot u \quad (1)$$

Where "k" being the coverage factor, 2 or 3 times the standard deviation is used to extend it to the standard 95-99% statistical coverage. Things become more complicated when we deduce the value we need from other measurement results in an indirect way (e.g., using a formula).

One of the possible ways to do this is a Type B determination. The situation is even more complex in the case of colour fastness tests because the response of a given specimen to the pre-treatment procedure can be obtained only once – which essentially means that this is a destructive test method. Naturally, we can make more specimens, but in this case, we immediately suspect that our measured characteristics are also influenced by the inequalities of the manufacturing process. Which makes it difficult to tell whether to what extent our own measurement process is responsible for uncertainty. And when the testing process is made up of many different, more or less controlled parameters, one cannot really neglect to carefully analyse how much these parameters can contribute to the swings of our measurement results.

In our case, we use Type B to determine measurement uncertainty because, after estimating uncertainties (U_A, U_B,… U_E) that cumulate during the test, they are considered as variance components and summed to determine the combined uncertainty (U). Context to determine combined uncertainty indexed by letter of test phases (A-E)

$$U_{combined} = \sqrt{(U_A^2 + U_B^2 + \cdots + U_E^2} \quad (2)$$

AN ALTERNATIVE WAY TO DEFINE MEASUREMENT UNCERTAINTY FOR COLOUR FASTNESS TESTING

In case of lacking scientific curiosity to determine the value of measurement uncertainty specifically for our research and our laboratory, or urgently need to provide an uncertainty value for a given test method, a less resource-intensive process is available due to international round-robin tests. Laboratories accredited for the tests in question shall participate in interlaboratory round-robin tests several times a year. The organizing institute provides the same sample (which is made of 100% wool in the case of this example) and then evaluates the submitted results. The statistical characteristics of the results submitted for a given test method (in this case, the colour fastness to perspiration) are evaluated by the type of adjacent fabrics and type of solution. After averaging the standard deviations of the more than 320 results classified by the adjacent fabric used, the overall value of standard deviation is 0,535. This can be converted into expanded uncertainty using Formula 3, resulting in uncertainty of 1,07 scale grades, with a 95% confidence interval. [9] As it is expected, this result would show a higher value than the value which is to be defined experimentally through the next chapters, specifically for our own laboratory. Naturally, as the total number of uncertainties in the 61 laboratories carrying out the round-robin test accumulates in this numeric value, in which different types of test devices, grey scales, adjacent fabrics, and laboratory staff may play a significant role. This makes the "responsibility" of our own measurement system very difficult to distinguish and define in terms of numerical values. Therefore, if appropriate resources are available, it may be more useful to quantify the value of our own system and keep track of changes in order to continuously improve the work of the laboratory.

SYSTEMATIZATION OF UNCERTAINTY COMPONENTS

To determine measurement uncertainty, we have broken down the process of colour fastness tests leading up to the measurement result as shown in Figure 2, since during these steps, the measurement result may be distorted, and the groups of measurement uncertainty components can be identified at these points. These factors will be included or omitted in our model of calculation, depending on their degree of relevance. The table in the annex summarizes the test parameters to be set up for the process. The sources of uncertainty in a particular test phase will also be these parameters. In the columns of the table, we classified the tracked parameters according to the different kinds of elements of the measurement system, and the colour codes indicate the classification of the factors in the critical analysis. This fully complies with paragraph 7.6.1 of ISO 17025:2017, which is one of the objectives of the research. [1] In addition to accurately monitoring the uncertainty parameters, the table provides the opportunity to illustrate the proportions of the factors based on the three pillars of the measurement system (i.e., calibrated and regularly checked measurement instruments, accredited suppliers, and proficiency of operators). Thus, in the event of a change of any of these factors, the table provides transparency in the exploration of causation and in the management of risks arising from measurement uncertainty.

DESIGN AND IMPLEMENTATION OF EXPERIMENTS ON CRITICAL FACTORS

Uncertainties in a particular process phase (see Figure 2) are that the error in the setting of a given parameter will also be a probability variable (temperature, duration of pre-treatment, the concentration of solutions, quantities added, amount of solution absorbed by the textile material, etc.). These random variations during the test process can escalate into smaller or larger differences in staining on the composite specimens when the results are compared to the greyscale. This is why the uncertainty of the final result is interpreted as a sum, that is, the sum of the uncertainties (as components of variance) generated in the previous steps of the process. (see Formula 2 – Figure 3)

In the course of our work, we had to examine these components of uncertainty about how they may increase uncertainty values. First of all, the laboratory's council of metrology examined at least critically – according to good engineering judgment – whether this factor could change at all and whether it could influence the results significantly or they can be logically excluded. At the meeting, we planned experiments on the suspected influencer factors. Where the practice or expert opinion is considered significant, we need to perform an experimental analysis.

- The process begins with sampling, where we have already found that, due to the inhomogeneity of the specimens obtained from the fabric, its ability to bind and release dye, as well as the resulting color change and staining, can be significant. Therefore, we decided to design an experiment for sampling differences between samples in the degree of uncertainty in scale grades.

- The pH range of the chemical content of sweat solutions to be prepared as standard is ± 0.2, which can be reliably adjusted on the indicator paper's colour scale, so the uncertainty of this factor is considered to be negligible and is not yet analyzed.
- Visual assessment on the pre-treated and dried samples based on the greyscale, is considered to be a significant component due to its key role.

Sampling uncertainty

The standard deviation of this factor was estimated from the differences (as ranges) between the results of the pairs of specimens treated with exactly the same treatment, and then the value of "U" was given. A total of 75 completely identical composite specimen pairs were subjected to fully standardized treatment. After averaging the ranges between the results of the pairs of specimens, the standard deviation was estimated by the following formula:

$$\hat{s}_{sampling} = \frac{\bar{R}}{d_2} = \frac{0{,}15}{1{,}128} = 0{,}133 \quad (3)$$

where the actual value of the statistical factor d_2 is 1,128. Based on this, the extended measurement uncertainty inherent in the sampling procedure is obtained using formula 4, by using the ranges between the results of two identical samples treated with the same procedure.

$$U = k \cdot s \quad (4)$$

This gives us the expanded measurement uncertainty for a 95% confidence interval (where k=2): $\mathbf{U_{sampling95}}$ **=0,266 grades**.

This verifies our idea that even with the highest degree of control over the testing process, the result may be significantly affected by the unevenness of the manufacturing of textiles. However, it is worth mentioning that as this value completely falls outside the control of the laboratory and the test method itself, including it within the final expanded uncertainty value could be arguable and debatable.

The uncertainty caused by visual assessment of staining - Gage R&R method

R&R analysis helps quantify the repeatability and reproducibility of measurement systems originally applied by automotive suppliers. Repeatability is the measure of the difference within a measurement sequence expressed in standard deviations. This can give you the difference in measurement results over a short period of time, leaving all elements of the measurement system intact. Reproducibility defines the vital differences between measurement sequences created in different circumstances (e.g., measuring person, instrument, location), also expressed in standard deviation. [10] Our aim is to quantify the accuracy with which the "measuring instruments" created by the eyes, experience, and judgment of operators can work together with the specific round-robin test methodology adopted by the automotive industry. After drying, the pre-treated specimens are visually evaluated using a nine-level greyscale (graded from 1 to 5 in half degrees) with colour differences as defined in ISO 105-A03. We compare the

difference between the standard adjacent fabric and the pre-treated specimen's staining with the shades shown in *Figure 1*.

We started with 12 samples of each of the 6 most common adjacent fabrics (cotton, wool, polyester, polyamide, viscose, and cotton used for testing fastness to rubbing). Each sample was graded 3 times with 3 operators, in random order to avoid the memory effect. Taking into account the results of all three operators on all types of adjacent fabrics, the repeatability of the measuring system (estimated standard deviation from the mean value of the ranges taken per operator) was 0,593 scale grades, its reproducibility (the standard deviation estimated from the mean result values of operators) was 0,275; thus **the R&R standard deviation value counts 0,654 grades of scale**. The latter value can also be used as a factor to estimate measurement uncertainty. Where there is a difference of opinion between two operators' results is the question of reproducibility; when one is not consistent with one's own results, it is a question of repeatability. It is clear from our numerical values obtained during the examination that the latter factor, in this case, contributes more than twice as much to the measurement uncertainty as to the former.

Since the color differences for each grade are non-linear, there is a much smaller, less perceptible difference between the intensities of staining at the better grades than the worse ones. In the future, it may be interesting to determine the varying detection accuracy. It would also be important to study this topic further because, in reality, the focus is not on the measurement results given by the grades but on whether the sample qualifies for a given certification, i.e., fails or passes. The average (reproducibility) and range (repeatability) control charts (well known from SPC and Gage R&R) show the overall uncertainty of the measuring system, as shown in the following figures. The horizontal axis shows the mean of the samples, while the vertical axis shows the average of repeated measurements and the ranges between such measurements.

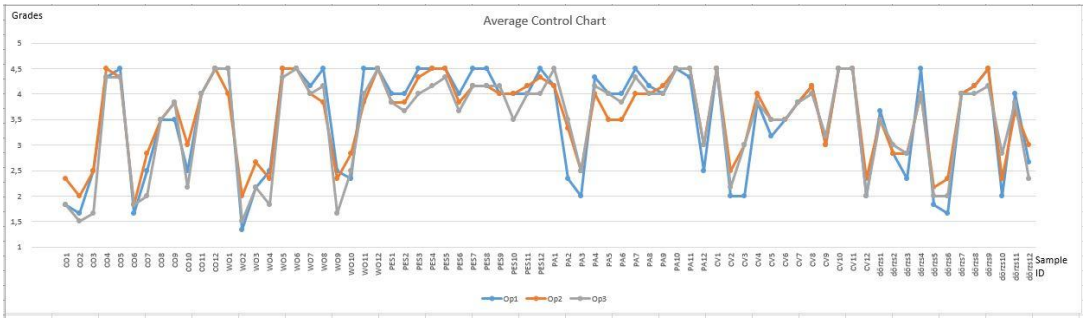

Figure 3: The "average control chart" to illustrate reproducibility

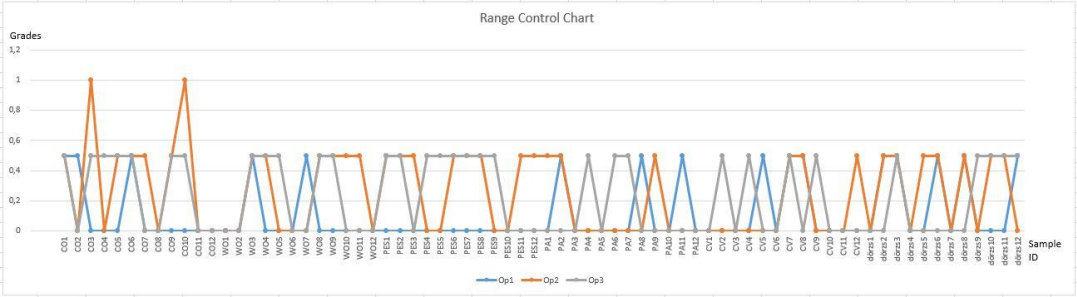

Figure 4: The "range control chart" to illustrate repeatability

DETERMINATION OF EXPANDED MEASUREMENT UNCERTAINTY

The combined standard uncertainty can be calculated using Formula 2:

$$U_{combined} = \sqrt{(U_A^2 + U_B^2 + \cdots + U_E^2} \ (2)$$

As there are only two uncertainty values were judged statistically significant during the experiments and left in the model, the combined expanded uncertainty can be represented by the following formula:

$$U = \sqrt{{U_{sampling}}^2 + {U_{visual\ assessment}}^2};\ U = \sqrt{0{,}266^2 + 0{,}654^2} = 0{,}706\ scale\ grades. \ (5)$$

We can state accordingly that the extended measurement uncertainty of colour fastness test procedures to water and perspiration in this laboratory counts 0,706 grades. Due to the high degree of similarity between the selected and examined factors, we can apply the established value to all colorfastness test methods in which we would be able to exclude any other factor of uncertainty except for sampling and visual assessment. As a further step in its development, the Council of Metrology has decided that the next step is to determine the sampling uncertainty of the colour fastness test to rubbing and to provide a more accurate uncertainty value based on the indicators of the special adjacent fabric used for rubbing.

SUMMARY

As mentioned above, currently, there is no systematic procedure to apply for measuring uncertainty for colour fastness tests, so in order to improve the method, our research has determined a measurement uncertainty that most accurately reflects the random variations caused by local conditions and techniques. According to the method now developed, we will identify uncertainty factors for further investigations, decide on their relevancy, calculate local uncertainty results as a component of variance, and consider them as a starting parameter for subsequent developments of the test method.

Color fastness to perspiration	Measuring instrument		Environment		Method		Measurand object		Operato	
A) Sampling							size of specimen	(40±2) mm x (100±2) mm	** It is the responsibility of the operator to monitor	
							adjacent fabric	in accordance with fiber	Legend:	
B) Solution making	Standard adjacent fabrics						ingredients of alkaline solution (/l):	0,5 g L-histidine 5 g sodium-chloride 2,5 g disodium-hydrogen ortophosphate-	could be a source of uncertainty	
	graduated cylinder						ingredients of acidic solution (/l):	0,5 g L-histidine 5 g sodium-chloride 2,2 g sodium-dihydrogen ortophosphate-	Guaranteed by the regular calibration of the measuring instrument/device	
C) pH adjustment	pH test paper						alkaline	pH 8 (±0,2)	ensured by the	
	0,1 mol/l sodium-hidroxide-solution						acidic solution	pH 5,5 (±0,2)	purchased from an accredited source/supplier	
D) Pre-treatment of specimens									trivial capability	
D1) Soaking			temperature	room	duration	30 minutes			object of measureme	
	glass rod	removal of excess liquor	liquor ratio	approx. 50:1	moving of the specimen	until evenly wetted				
D2-D3) Pressure and thermal treatment	perspirator		temperature	(37±2) °C	duration	4 h				
	glass/acrylic sheet		pressure	(12,5±0,9)						
	drying oven									
D5) Drying	clothespin									
	drying oven		temperature	max. 60 °C	suspension	contact of layers				
E) Visual assessment	colorimeter OR		source of light	D65	angle of observation	approx. 90 °				
	the naked eye and		illumination	min. 600				color change of		
	standard adjacent							staining on the		

* - Parameters defined by the standards but unusual and/or exceptional are not covered in this table; it is only intended to provide a general overview of the uncertainty components that occur during the testing process.

Figure 4: Table of uncertainty factors for colour fastness to perspiration [5]

REFERENCES

[1] ISO/IEC 17025:2018 – General requirements for the competence of testing and calibration laboratories

[2] ISO 105-A01:2010 - Textiles. Tests for colour fastness. Part A01: General principles of testing

[3] ISO 105-A03:1987 – Textiles. Tests for colour fastness. Greyscale for assessing staining

[4] ISO 105-E01:2013 – Textiles. Tests for colour fastness. Part E01: Colour fastness to water

[5] ISO 105-E04:2013 – Textiles – Tests for colour fastness – Colour fastness to perspiration

[6] JCGM 100:2008 – Evaluation of measurement data – Guide to the expression of uncertainty in measurement

[7] EA-4/16 G:2003 – EA Guidelines on the expression of uncertainty in quantitative testing

[8] ILAC-G17:2002 Introducing the Concept of Uncertainty of Measurement in Testing in Association with the Application of the Standard ISO/IEC 17025

[9] Testex Rundtest – Colour Fastness No. 57. Evaluation (Revised Version) (09.2019)

[10] AIAG: Measurement Systems Analysis (MSA), 4th edition

QUANTIFYING RISK OF CLASSIFICATION OF PROTECTIVE TEXTILES USING MEASUREMENT UNCERTAINTY

Tibor GREGÁSZ, Veronika PÁL

Abstract: *Laboratories executing performance testing of protective textiles (e.g., CE marking of protective gloves) are obliged to evaluate measurement uncertainty. Currently, this is a challenging task due to the complexity of test methods. In our research, we define this parameter using a newly implemented model of error propagation and use it to assess the risk of performance level classification, which can be interpreted as the proportion of products failing to reach the expected limit value.*

Keywords: *TDM test method, measurement uncertainty, error propagation model, CE marking*

INTRODUCTION

Conformity assessment of protective gloves against mechanical risks includes determination of resistance to cutting by sharp objects (TDM test method), which is described by the standard ISO 13997:1999. The protective equipment's level of performance is defined and classified by the test results. Limit values concerning this product type are specified in the standard EN 388:2016.

The previously unspecified uncertainty values which have been determined during our research are not only informative but also can be used as an indicator of the test method's efficiency as well as for the improvement of components of the measuring system.

THE TEST METHOD AND ITS MEASUREMENT UNCERTAINTY

Principle of test method [1]

One of the appropriate methods is described by the standard ISO 13997:1999, which defines its result by the force that is required to be applied perpendicularly to a blade to cut through the protective material in a blade stroke of length 20 mm.

- After the specimens are mounted on a curved specimen holder, the intact part of the blade is pushed forward while a specified force is being applied to it.
- A blade sharpness correction factor has to be calculated for blades of the same batch by cutting a neoprene calibration material.

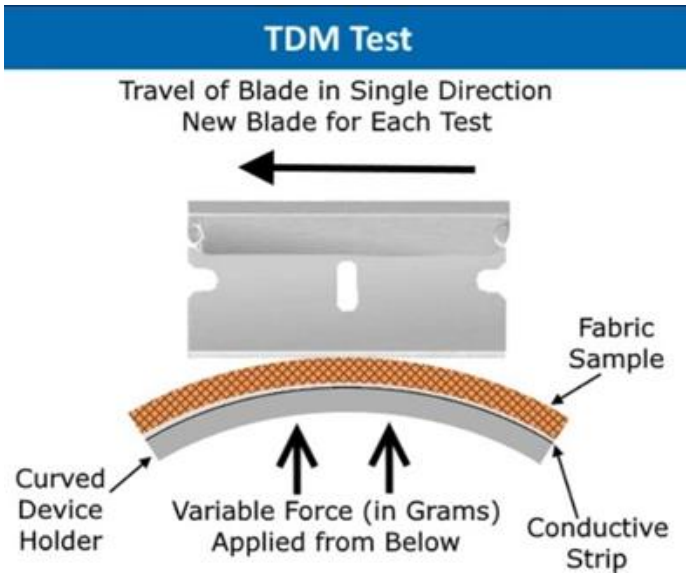

Figure 1: Schematic drawing of the execution of TDM test method

- Test results are multiplied by the correction factor of the respective batch of blades, determining "normalized cutting stroke lengths". Theoretically, this makes the results comparable with each other, regardless of the manufacturing characteristics of the blade batch. Then, the test procedure continues mostly graphically.
- Normalized cutting stroke lengths are placed on a diagram as a function of the pressure force applied.
- Consequently, the best-fit regression curve is chosen and drawn. (According to the current standard test method, this is a free choice, although a factor of uncertainty in itself.)
- In two turns, adding data from new measurements for improving statistical reliability, the cutting force at the cutting force length of 20 mm is determined using the regression equation of the curve.
- The level of performance of the protective equipment under examination can be defined using this value, following the limit values prescribed in a table of the harmonized standard.

Contributions to measurement uncertainty and error propagation

Measurement uncertainty is a parameter that is bound integrally to the result of the measurement and shows the natural variance of the series of measurements around the true value of a quantity.[4] According to ISO/IEC 17025:2017, an accredited laboratory shall analyze and evaluate (but at least estimate) all significant contributions to measurement uncertainty of each and every test procedure used, using an appropriate method. [2]

If test results are given indirectly, using several different measured values and arithmetic calculations (e.g., determination of density by dividing the results of the mass and volume measurements), the error of each measurement result propagates to the calculated results. Using

[4] JCGM 200:2012 International vocabulary of metrology – Basic and general concepts and associated terms

the function which specifies the correlation between input values and outputs makes it possible to define the result's deviation caused by the change in input values (in this case, the value of random error). The propagation of the *u* values during the test procedure can therefore be monitored by means of differential calculus. [3]

Interpreting the measuring system of the TDM method as a theoretical measuring element

Distinct units of the measuring system can be summarized as follows:

- specimen holder with the specimen mounted and a circuit detecting cut-through of the specimen,
- blade cutting through the specimen,
- force application system providing constant force between the cutting edge and the specimen,
- cutting-motion system moving the specimen holder and the cutting edge relative to each other and a cut-stroke length measurement system.

To determine the measurement result (as it is described in Chapter x.y), individual series of measurements are performed executing cutting using different forces of the load to achieve cut-through. During the procedure, readings are being done about the length of displacement required to perfect cut-through (dependent variable). Due to the reasons previously described, these lengths show variance, meaning the final result of the measurement is a value of distance, which is the sum of cutting stroke length and random errors at a distinctly set force value. By marking direct measurement results with data points in the diagram, cutting stroke lengths are assigned to the distinct values of force (see regression diagrams later on).

The model of operation of measuring transducers can be represented by a regression curve, reflecting a clear relationship between the set (x) and resulting (y) values. The regression diagram defined should be interpreted as a static characteristic of a transducer's behaviour. In the case of the TDM test method, on account of the velocity of the movement of the cutting edge (2,5±0,5 mm/s) the measurement process is just quasistatic, but this is considered to be one of the disregarded measuring conditions which may be scientifically examined later on but is a fixed data currently due to the standard test method.

Therefore, the "behavior" of our measuring system is expressed by a characteristic curve. To analyze the question, we should consider and use this equation as the "black box" of the measuring system, avoiding the detailed analysis of technically identifiable uncertainty contributions individually.

Identifying the basic concept of the problem

Following the standard principle of testing procedure: "The sample's resistance to cutting by sharp objects is expressed by a cutting force, which is required to be applied to a blade to just

cut through a material in a blade stroke length of 20 mm."[5] The sample to be qualified is classified by levels of performance based on this cutting force.

However, cutting force is determined indirectly, using the depiction of cutting stroke lengths produced by different loads and their regression function. Therefore each and every measured value is influenced by all uncertainty contributions caused by the parts of the measuring system.

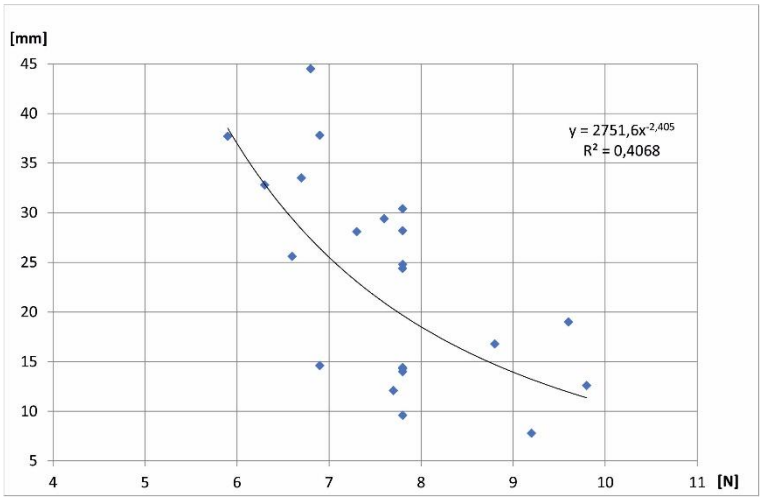

Figure 2: Diagram of the measurement results of a TDM test procedure, with a power regression curve

CALCULATION OF UNCERTAINTY OF THE TDM TEST METHOD USING ERROR PROPAGATION MODEL

In our research, the cumulative effect of each factor is quantified by determining the test procedure's combined measurement uncertainty.

To define the value of standard uncertainty (u) and the risk of classification, the following steps were specified by our method.

- 1./ Determination of cutting stroke lengths as a function of a certain load force, using the respective batch of blades on the neoprene calibration material.
- 2./ Using the cutting stroke lengths carrying uncertainties, the standard uncertainty ("u") propagating to the correction factor is determined.
- 3./ Multiplying cutting stroke lengths measured on the test specimen and the known correction factor (which is subject to error) gives the standard uncertainty of linearly connected cutting stroke lengths.

[5] ISO 13997:1999 Protective clothing — Mechanical properties — Determination of resistance to cutting by sharp objects

- 4./ Knowing the standard uncertainty of normalized cutting stroke lengths, applying the model of error propagation, the uncertainty of the pressure force originating from the regression curve at a given constant (20 mm).

When expressing uncertainty, the basic concept is that the results of length measurement and their content of error at a set load force follow a mathematical distribution due to their randomness. On account of the complexity of the manufacturing processes of the blades, the neoprene and the test samples to be measured on the one hand, and given the various distortive effects of the measurement process, on the other hand, it is safe to assume that in case of a larger number of influencing factors the central limit theorem applies. [4] Taking this into account, measurement results approach a normal distribution. Measurement uncertainty, which can be identified as the random error of measured values, should be a good estimate to be considered equal. However, according to the test procedure's present conditions, this range is estimated through the residual standard deviation of the points deviated from the known regression curve. Naturally, this assumption must be tested with accurate analysis in a validation procedure.

- One of the two factors is the determination of the correction coefficient, in which case the variance of the blade and the calibration neoprene applies.
- The other factor is the measurement series performed on the specimen, where the deviations are caused by the variance of the blade and the test sample.

Therefore, the deviations originated from the previous two factors will be propagating as the random error throughout the calculations performed during the evaluation of the measurement results, as it is prescribed by the test method. Finally, these deviations sum up as the value of combined measurement uncertainty.

An error of the correction factor's determination

The correction factor is defined by repeated measurements, whereby random deviations of the measuring instrument (blade) and the measurand (calibration neoprene) applies the same way as it was stated before. Also, other incidental uncertainty contributions might have an impact as well, so the correction factor possesses its own measurement uncertainty. The correction factor of the respective batch of blades is calculated by using the following equation:

$$C = \frac{20}{\overline{l_C}}$$

where

- C is the correction factor [-],
- $\overline{l_C}$ is the average of the measured cutting stroke lengths [mm],

Indicating the measured data (which was acquired by a previous calibration of a blade batch) as a function, it is apparent that the standard deviation (s) of the measured cutting stroke lengths

- meaning their Type A standard uncertainty (u=s) - inflicts a quantifiable uncertainty in the value of the correction factor.

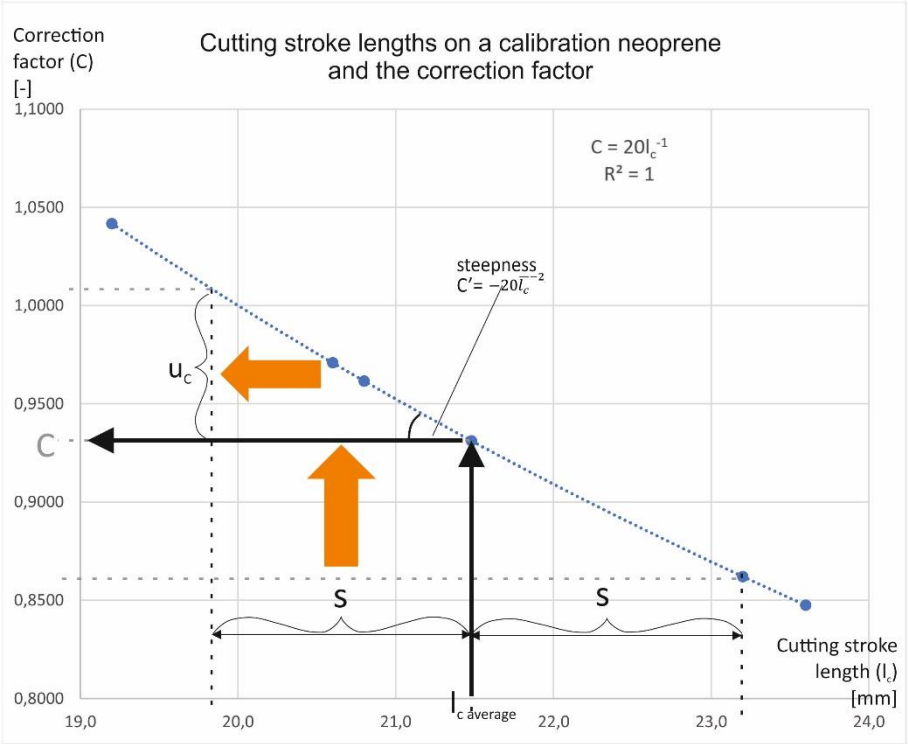

Figure 3: Error propagation applied to the determination of the correction factor (example)

According to the model describing the correlation, the standard deviation of cutting stroke lengths causes a standard uncertainty propagating to the correction factor, depending on the slope of the function. The slope of the function (thus the extent of propagation) is defined by deriving the regression curve:

$$C = 20 \cdot {l_c}^{-1}$$

$$C' = -20 \cdot {l_c}^{-2}$$

As a result, the standard uncertainty ($\boldsymbol{u_C}$) of the correction factor originated from the measured lengths is defined by the following equation:

$$u_C = s_l \cdot (-20\bar{l_c}^{-2})$$

An error of the determination of normalized cutting stroke lengths

Normalized[6] cutting stroke lengths (l_n) are defined following the test procedure: the measured and recorded cutting stroke lengths (l_m) are multiplied by the correction factor indicating the sharpness of the blade (C), meaning

$$l_n = l_m \cdot C$$

According to our estimations, the value l_{meas} displayed by the measuring device is not subject to significant error on the part of the measuring equipment or the environment. However, the standard uncertainty of the preciously determined correction factor (u_C) propagates linearly to the normalized cutting stroke lengths, as it is shown on the figure down below.

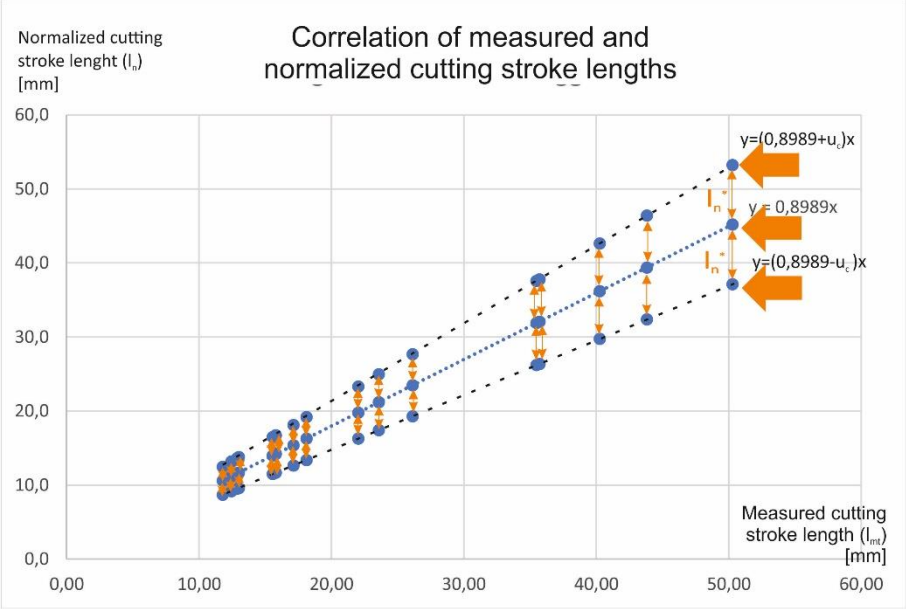

Figure 4: Propagation of error of the determination of normalized cutting stroke lengths

The l_n'values subject to error are define by the following equation:

$$l_n^* = (C \pm u_C) \cdot l_m$$

The values l_n^* and l_n change linearly, therefore the uncertainty of determining the normalized cutting stroke lengths is identified by averaging the elements on both ends or the known ones in between (u_{ln}):

[6] Normalization of cutting stroke lengths means multiplying by the correction factor, according to the terminology used in ISO 13997:1999.

$$u_{ln} = \frac{\sum_{i=1}^{n} |l_{ni}^{*} - l_{ni}|}{2n}$$

This random error is estimated by the measurements of the correction factor and can be considered general; it propagates to each and every normalized cutting stroke length. When estimating $u_{ln,}$ only half of the absolute linear deviation values are taken into account, as the extent of the variance here includes deviations further from the regression curve.

Regression curves and the related calculations

According to the standard procedure, the best fit curve shall be drawn of the force-cutting stroke length point pairs, which enables to calculate of the cutting force at a cutting stroke length of 20 mm.

The regression equation represents the correlation between the load force and its inflicted cutting stroke length, as it has been elaborated at the idea of the theoretical measuring transducer. Therefore, during the following steps of the test procedure, our calculations will be based on this function (as a conceptual static characteristic), using the possibilities given by the model of error propagation on uncertain variables and the connecting uncertainty values.

When the model of error propagation was being made, an example of a frequently used power function was used. Nevertheless, by using the following method, the principle presented can be applied to other functional relationships as well.

Uncertainty of the regression curve

As the next step of the test procedure, we need to quantify the deviations ("errors") compared to the regression curve to represent the variation of measurement results on the final test result. For this purpose, the residual standard deviation (S_r) of the experimental pair of value is used, which is calculated by using the following equation:

$$S_{r1} = \sqrt{\frac{\sum_{i=1}^{n} (l_{ni} - \widehat{l_{ni}})^2}{n-2}}, \text{ where}$$

- l_{ni}normalized cutting stroke lengths determined by "real" measurements (indicating as a function of load force used for the measurement),
- $\widehat{l_{ni}}$ the cutting stroke lengths belonging to the respective load forces, estimated by the regression equation
- n the number of measurements.

The uncertainty components expounded in the previous chapters (l_n and C) are randomly combined, therefore, their standard deviation sums up given the square root of the sum of their variance. That is why the combined uncertainty of the regression curve ($\boldsymbol{u_{r1}}$) arises from the sum of squares of the two deviation values:

$$u_{r1} = \sqrt{{u_{ln}}^2 + {S_{r1}}^2}$$

The u_{r1} value continues to be expressed in the dimension of cutting stroke lengths [mm].

The propagation of the error of cutting stroke lengths onto the cutting force

The test procedure's following step is to calculate the cutting force value belonging to a cutting stroke length of 20 mm, using the regression curve. This propagates the random error applicable to the previously determined cutting stroke lengths, to the value of the cutting force. The way to do this is also determined by the functional relationship described by the equation.

In the series of test procedures that were used as an example for our analysis, the approximation was made with a power function, so the general equation of the correlation (Fv still indicating the cutting force and lsz stands for cutting stroke lengths): Parameters *a* and *b* apply to the respective test samples in question in case of a power regression.

$$F_1(l_n) = a \cdot {F_v}^b$$

The figure below illustrates through the measurement results of an actual TDM test procedure how the deviation (u_r) determined on the vertical axis is projected on the horizontal axis. The error arisen on axis y propagates to axis x. The steeper the part of the curve coming from the y-axis (subject to an error of a given size), the smaller the error propagating to the x-axis will be. Consequently, if we know the measurement uncertainty of the input characteristic (cutting stroke length) (u_r), and the steepness of the curve -*l(F)*'-, we are able to calculate the output characteristic's (cutting force) error and standard uncertainty (u_{Fv1}).

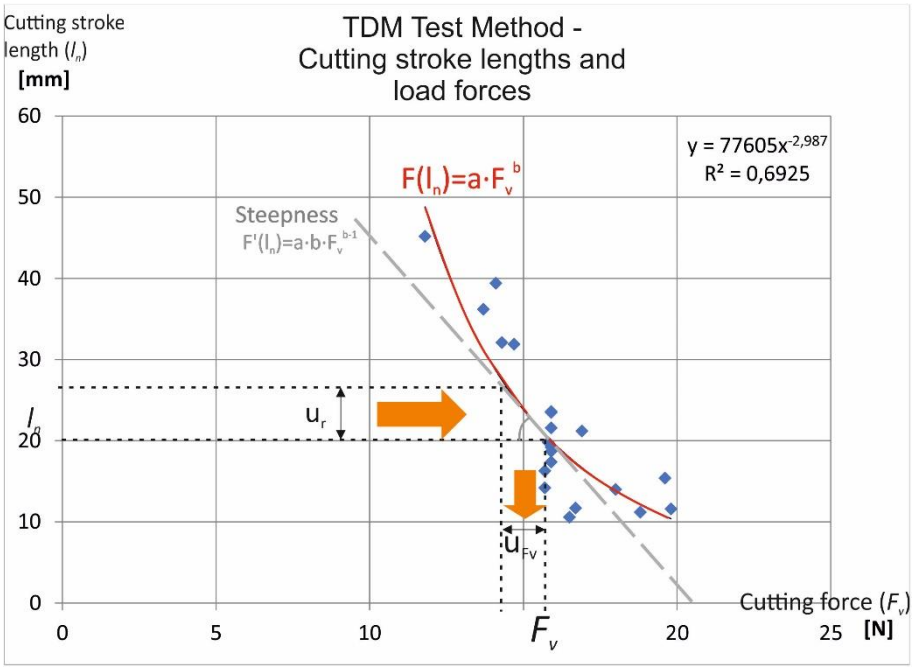

Figure 5: Example of error propagation on the regression curve

By deriving the regression function, we get the equation describing the slope of the curve at the point in question:

$$F(l_n) = a \cdot {F_v}^b$$

$$F'(l_n) = a \cdot b \cdot {F_v}^{b-1}$$

Using the slope and rearranging the equation the uncertainty of the cutting force is the following ($\boldsymbol{u_{Fv}}$):

$$u_{Fv} = \frac{u_r}{a \cdot b \cdot {F_v}^{(b-1}}$$

where

- u_{Fv} is the uncertainty of the cutting force belonging to a cutting stroke length of 20 mm [N],
- u_r is the combined uncertainty of the regression curve [mm],
- a and b are the coefficients of the regression equation,
- F_v calculated cutting force at the cutting stroke length of 20 mm [N].

Regression curve supplemented by the new measurement results

After using the curve drawn first, we determined the cutting force; we have to perform another 5 or 10 measurements with the given load, which, in addition to the results shown above, we need to determine the cutting force again at 20 mm using a refined regression curve. This will be the final result of the test procedure.

In the case of redrawing the refined, more precise regression curve, we have to recalculate the u_{ln} associated with the determination of the normalized cutting stroke lengths, as well as the residual standard deviation of the new curve (S_{r2}). Therefore the combined uncertainty (u_{r2}) of the second regression curve will be given by the sum of squares of the two previous factors:

$$u_{r2} = \sqrt{{u_{ln2}}^2 + {S_{r2}}^2}$$

The u_{r2} value is expressed in the dimension of cutting stroke lengths [mm].

Measurement uncertainty of the final result

The final result of the test procedure is given by the cutting force belonging to a cutting stroke length of 20 mm. As the last step of the application of the model of error propagation, in accordance with Chapter x.y, the combined uncertainty of the regression curve shall be projected to axis x as described above, using the following equation:

$$u_{Fv2} = \frac{u_{r2}}{a_2 \cdot b_2 \cdot F_{v2}^{(b_2-1}}$$

The value obtained (u_{Fv2}) is the Type A, combined measurement uncertainty value, specific to the particular test sample and test.

RISK OF PERFORMANCE CLASSIFICATION

Based on the combined measurement uncertainty value (u_e) calculated by the above-mentioned model of error propagation, we have made further suggestions regarding the application of the result (Besides being an obligation for accredited laboratories)

This value can also be used in the course of the classification of the tested protective equipment according to the performance level by a probability risk model. This is because the test result is also a probability variable, and according to an earlier train of thought, this will also deviate according to normal distribution around the designated force value. As the deviation can be interpreted as the previously defined standard uncertainty (u_e), limit values of the performance levels can be shown and visualized on the same diagram as the probability density function.

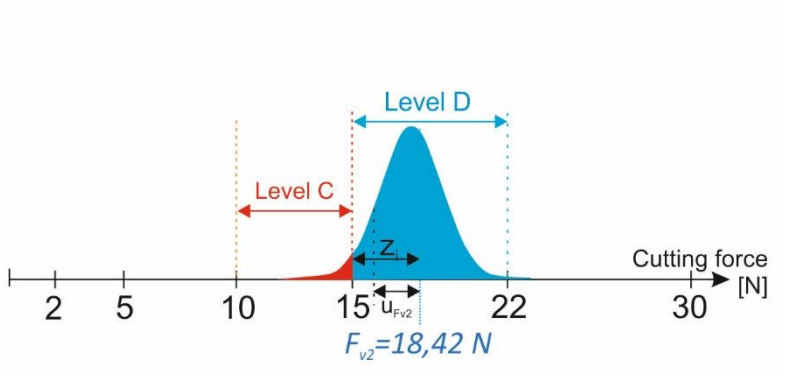

Figure 6: The expected ratio of products that are non-compliant (red) with their level of performance due to their test results and uncertainty values (see performance levels in EN 388:2016)

In this case, we only take into account the lower limit value of the result (to its left), as it is a question of product certification of protective equipment. The risk is now identified with the probability of the product not reaching the lower limit of the given performance level, posing a threat to the user.

The limit value (F_{min}) between level C and D is at 15 N. As an example, a test result (F_{v2}) of 18,42 N is given as the average, and its combined measurement uncertainty (u_{Fv2}) is at 2,31 N. To define the normalized z_i value:

$$z_i = \frac{F_{v2}-F_{min}}{u_{Fv2}}; \text{ i.e. } \textit{-1,48-}$$

Based on the value of z_i, the probability (given by the distribution function) to not reaching 15 N is 1-0,9306. Therefore the risk of misclassification of the tested product regarding the category of 15-22 N is 6.94% – in case the representativeness of the sample was provided. [5]

SUGGESTIONS AND FURTHER OBJECTIVES

When developing the test method (and the standard), it is worth simplifying the procedure for evaluating the results. Of course, this decision would require further consideration of aspects.

It is essential to assess the effect of the chosen type of regression curve on the final result, its uncertainty, and the classification risk, as the choice of curves is not sufficiently regulated at the moment for laboratories.

In case it is possible to identify the proportions of individual uncertainty components – for example, which part of the combined u value is caused by the blade and which is caused by the internal variance of the test specimen –, more accurate conclusions can be drawn regarding the test result's evaluation procedure.

REFERENCES

[1] ISO 13997:1999 Protective clothing — Mechanical properties — Determination of resistance to cutting by sharp objects

[2] ISO/IEC 17025:2017 General requirements for the competence of testing and calibration laboratories

[3] JCGM 100:2008 Evaluation of measurement data – Guide to the expression of uncertainty in measurement

[4] Lukács O. (2006): *Matematikai Statisztika*, Műszaki Kiadó, Budapest (ISBN 963-16-3036-6)

[5] Koczor Z. et al. (2012): *Anyagszerkezettan*, Óbudai Egyetem, Budapest

IMPACT OF THE COVID-19 CRISIS ON TEXTILE- AND GARMENT INDUSTRY SECTOR WITH FOCUS ON CEE AND WB COUNTRIES

Edit CSANÁK, Ineta NEMEŠ, Anita SÓS

Abstract: *Covid-19 crisis has a significant impact on the textile and fashion industry worldwide. The impact of the coronavirus pandemic on textile manufacturers has been unprecedented. According to the latest reports, reducing sales, closed factories, and lower wages are just some of the problems. The economic downturn associated with the COVID-19 epidemic has posed challenges to the textile, clothing, and footwear industries. Companies, brands, and designers fight for their survival. This article attempts to give insight into some general facts of the impact of the COVID-19 pandemic on the textile- and garment industry sector worldwide and in some of the Central East European and West Balkan countries.*

Keywords: *COVID-19 crisis, garment industry, textile industry, CEE, and West-Balkan Countries*

INTRODUCTION

COVID-19 is an infectious respiratory disease caused by a coronavirus that presumably started in September 2019 from Wuhan Province, China. Coronaviruses are spread among animals but can also infect humans. Overall, COVID-19 is the name of a new human epidemic created by the new coronavirus worldwide, which can cause fever, fatigue, cough, breathing difficulties, and even death. The coronavirus pandemic's negative economic effects around the world are unquestionable, and the impact of the coronavirus pandemic on the textile and fashion industry and the manufacturers has been unprecedented. This article attempts to introduce the critical information to give insight into some general facts of the impact of the COVID-19 pandemic on the textile- and garment industry sector in some of the Central East European and West Balkan countries.

GLOBAL ECONOMIC IMPACT OF THE COVID-19 PANDEMIC ON THE TEXTILE AND FASHION INDUSTRY

Over the past 10 years, world trade has grown by an average of 4.8% and total world GDP by an average of 1.6%. In 2020, however, the OECD forecasted a 15% decline in world trade volumes. A similar fall was also exemplified by the Great Depression and the 2008 crisis.

The situation has been twice as severe in history, once during the World Economic Crisis of 1929-1930, when it affected 83.8% of the countries. During the World Economic Crisis of 2008, it affected 61.2% of the countries and caused a significant economic downturn. The acceleration of globalization can explain the current high level of involvement.

According to Lacy Hunt's summary, the IMF, or World Bank, estimates that 92.9% of countries globally will go into recession by 2020. [1] (Fig. 1)

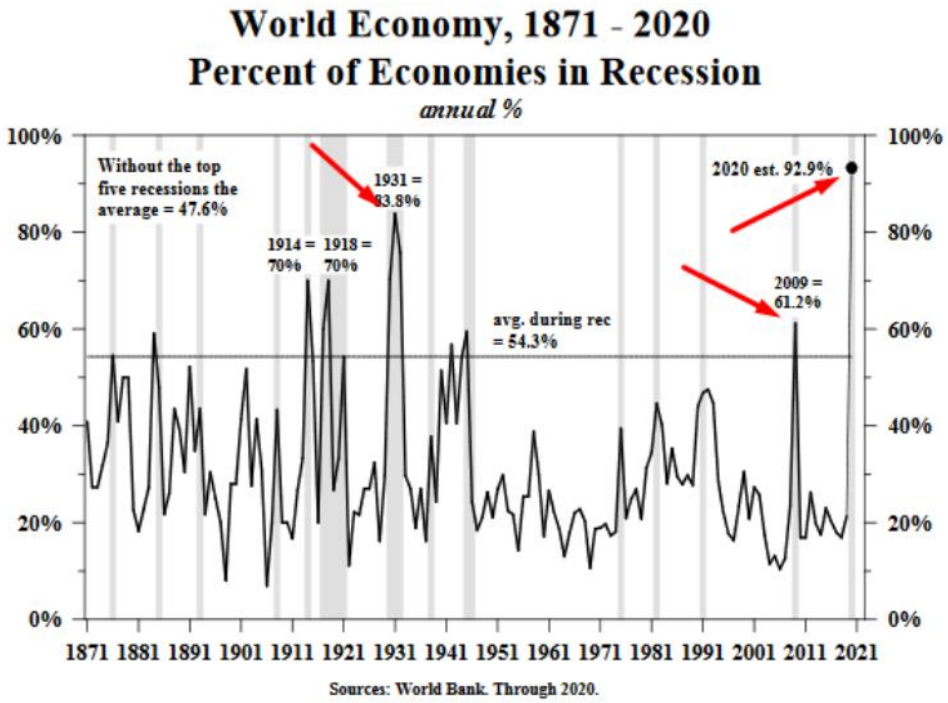

Figure 1: Diagram of economic recession according to Lucy Hunt's summary

Globally, many people have lost their jobs[7], countless businesses have gone bankrupt, and the presence of a pandemic has caused people to feel generally unwell and worried. Some economic sectors were made entirely impossible by the closure of national borders, but economic areas could quickly adapt and operate during the epidemic.

Figure 2: (Left) A woman sitting near sewing machines in a recently closed garment factory in Myanmar to demand her salary; (right) Illustration

[7] In Cambodia, however, the law requires employers to ask permission from the government to lay off workers, and they would be required to pay 40 percent of the minimum wage there for half a year to workers, but locals say this is not the case and they have not even received their pay. (See: Fig. 4) (Source: The Guardian) [11]

The pandemic's harmful effects have hit tourism and the fashion and luxury goods market hardest, where consumption has fallen dramatically due to their so-called non-essential nature. In contrast, the demand for health and hygiene products needed to meet our basic needs and food consumption showed a slight increase.

The changes are also affecting our daily lives, and the looming economic recession will have a significant impact on our shopping habits. *"From Chinese raw material production to online commerce, the impact of the coronavirus is also being felt in the clothing industry. Besides, the downturn is coming in more waves and will hit the most vulnerable hardest: developing countries and producers with ever-smaller margins."* [2]

The International Labor Organization (ILO)[8] estimates that 65 million people work in the textile and clothing industry in the 10 countries most concerned with the textile industry.[9] Furthermore, an ILO study points out that the global textile trade collapsed in the first half of 2020. On the one hand, because of the main purchasing region's needs, the EU, the United States, and Japan have fallen by 70%. On the other hand, the supply chain has already collapsed at the production level due to a lack of cotton, material, and other necessary equipment. [3] The figure below shows the percentage of textile and clothing purchases in the 6 main import countries by the 3 main importing countries, i.e., the EU, the USA, and Japan, paralleled to the same month of the previous year. Demand had already fallen drastically in April, and the situation has only worsened since then.

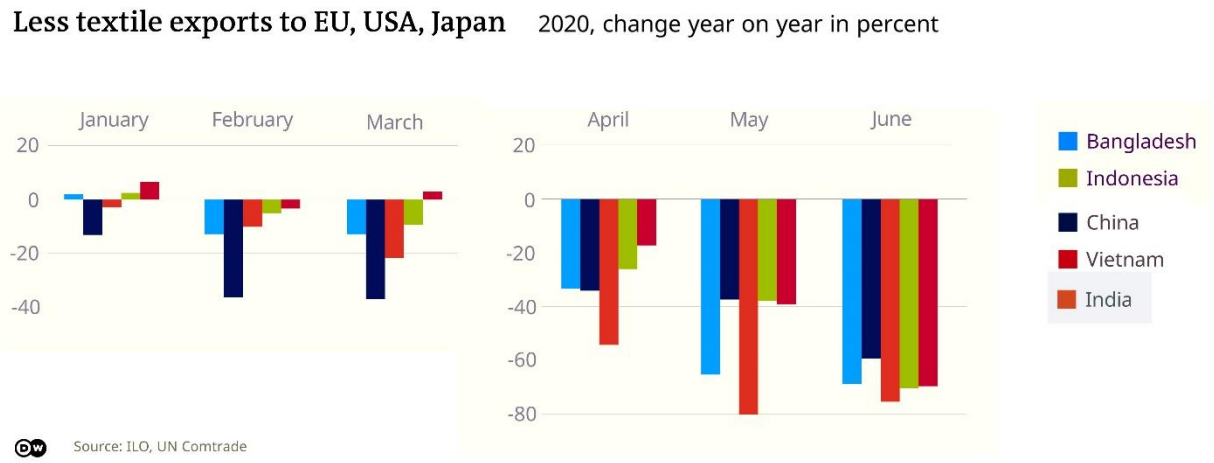

Figure 3: Declining export chart

When the virus exploded, clothing manufacturers and suppliers worldwide faced the cancellation of completed or near-completed orders. A study of 500 garment manufacturing facilities found that 86% of these companies were affected by canceled or pending orders. As a

[8] Organization of the United Nations

[9] Namely Bangladesh, Cambodia, Pakistan, Sri Lanka, Myanmar, Vietnam and China. , India, Indonesia, and the Philippines

result, 40% of the companies have difficulty paying workers 'wages, leading to mass redundancies and factory closures. As these are the poorest countries globally, the livelihoods of many people have been put at risk. However, even in this situation, consumers expect brands to adhere to their ethical commitments. Furthermore, in a 6,000-person study that found responses from, among others, American, English, Italian, German, and Chinese consumers, they favored companies that paid for laid-off workers or redesigned their manufacturing processes to make health equipment for workers, or and donated to the community. Also, environmental programs were evaluated by the respondents. [10] [4]

"The pandemic has exacerbated pre-existing inequalities," the ILO report assumed; before the pandemic, women – even worked longer hours – were typically paid less than men.

Figure 4: Garment workers in Bangladesh's capital Dhaka took to the streets to demand payment of wages in May; police later dispersed them

The probable impact of the COVID-19 epidemic in 2020 on global fashion and luxury product sales is hard to estimate accurately. However, after a low of 59-68% in April, an improvement has been forecasted for the end of the year. An average decrease of 28-38% is expected for 2020 compared to 2019 sales. Experts estimate that the global fashion industry (clothing and footwear sector) will fall by 27-30% compared to 2019, although the industry is projected to grow by 2-4% in 2021 compared to 2020. If stores remain closed for 2 months, McKinsey's analysis will put 80% of listed fashion companies in Europe and North America in financial trouble, suggesting that many fashion companies will go bankrupt in the next 12-18 months. [5] [6] Also, the expert predicts that the only way to secure survival is e-commerce. The development of the companies' digital abilities and tools can boost the fashion industry if the Covid-19 takes to hold. [7]

[10] Apparel Coalition: Weaving a better future: Rebuilding a more sustainable fashion industry after Covid-19

LATEST UPDATES ON THE IMPACT OF COVID-19 CRISIS ON THE EUROPEAN GARMENT SECTOR

In the matter of latest updates on the impact of COVID-19 crisis on employment and Government measures in some of the Central East European and West Balkan countries, the latest reports show that *"a complete recovery is still uncertain, despite some positive signals – the latest economic data show."* [8]

General information on the Hungarian Textile and Garment Industry (HGTI)

The Hungarian textile and garment industry (HTGI) has been in a problematic situation for more than a decade. The first problems occurred around 2005 when imports of cheap Asian textiles and clothing increased significantly. It was followed by symptoms of mushroom-growing second-hand shops around 2008-2010. Some corporations have become so strong that they have also become essential taxpayers in the country.

According to the latest available information (2019), the Hungarian textile industry:

- Employees (persons): 7316
- Production value: Nearly 400 million euros
- Number of registered enterprises: over 2600

According to the information available from 2019, the Hungarian clothing industry:

- Employees (persons): over 20 000
- Production value: nearly 300 million euros
- The number of registered enterprises: over 4000

Latest updates about the impact of the Covid-19 crisis on the HGTI

A non-representative survey conducted by the Hungarian Light Industry Association in April 2020 analyzes the Coronavirus economic crisis's impact on the domestic textile and clothing sector (SMS's). According to this statement, most responding companies are engaged in clothing production in the domestic textile and clothing sector. [9]

- Almost half of the respondents employed less than 10 employees. The companies, which employ 50-250 people, mostly came from companies that manufacture textiles and clothing accessories.
- The challenging export-import activity affected about half of the respondents. The share of companies providing contract work services was about 35%.
- 92% of the companies surveyed were severely affected by the coronavirus situation. Missing or canceling orders affected 90% of companies, and also, the decline in sales.
- 50% of them complained about the lack of access to local partners.
- 55% complained of increased raw material prices and were struggling with a shortage of raw materials.

Companies further complained about:

- Receipt and payment of ordered and manufactured products.
- Loss of domestic audience due to shopping malls being closed.
- Liquidity problems due to canceled orders are among those who are not engaged in the production of fashion goods but the production of uniforms and clothing supply for special events.
- Some were unable to function due to the workers' illness, problems in the textile supply chain, and logistical problems.

According to the analysis made by the State Audit Office analysis, The Government's response to the labor market crisis, which also affected the textile industry, was useful. The 5 most important measures:

- Tax relief and deferred payment on social security obligations;
- Tax and contribution reductions in specific sectors;
- Job protection and Job-creating wage subsidies;
- Increasing government orders;
- Soft loans.

Despite all this, half of the companies planned to reduce production and 20% to downsize altogether and close down the business.

Vision and future perspective of the Hungarian companies and representatives

Regarding the data of the non-representative survey, half of the interviewed respondents have a positive vision. They design to implement the following steps:

- Changing the supply chain
- Identifying new markets
- Temporary reduction of the workforce
- Reducing product workflow and manufacturing
- Switching to other products
- Introduction of online sales, webshop development

The measures taken to improve the Hungarian light industry's situation in Hungary are coordinated jointly by professional organizations, including the Hungarian Light Industry Association, the Textile Industry Technical Association, and the Hungarian Fashion and Design Agency. They have a dialogue with the Government. I'm involved in the Vocational Training Development Workshop of the Hungarian Fashion and Design Agency.

These organizations provide online training (HFDA Academy), do surveys, and coordinate start-up programs. The VOCATIONAL TRAINING 4.0 legal regulation changes, which came into force in the autumn, pose severe challenges for all sectors. It is also an opportunity. To ensure the success of human strategy developments in the domestic textile and clothing sector, the Government conducts consultations through these organizations, involving the Higher Education Institutions and the Vocational Training Office.

Information about the Serbian garment and textile industry sector (SGTI)

Textile and apparel production in Serbia has a long-standing tradition and, for many years, has been one of the leading export industries of the country. Nowadays, around 1800 active companies with more than 43 000 employees operate in the Serbian textile, according to data by the Development Agency of Serbia (RAS).

In 2014, the textile sector's export in the country reached a value of 1.2 billion dollars, which was a rise of about 8% compared to the previous year. The textile production and garment industry generated USD 853 million or 72% of this export, representing a rise of 7% compared to the same period in 2013. From 2001 to 2014, the growth of exports for the textile and clothing industry in Serbia rose from USD 228 million to a staggering USD 853 million, representing a growth rate of over 374% in 13 years. Heavy- and light garments, knitted garments, sportswear, jeans, children's clothing and baby equipment, work clothes, uniforms, underwear, socks, home textiles, and carpets; only some of the programs of Serbia's textile and clothing manufacturing industry capacity. Garment workers in Serbia[11] are said to be earning less than a living wage producing clothes for German fashion brands – with many having to carry on despite the Covid-19.

According to the Serbian Chamber of Commerce, the drop in production of the SGTI caused by the COVID-19 pandemic in April amounted to 62% compared with the same month last year. From the beginning of May, production began to return to normal, so that currently all producers can work at full capacity. [10]

CONCLUSION

The COVID-19 pandemic had disrupted the European textile and apparel industry like never before and significantly impacted the textile and fashion industry worldwide. The economic downturn has posed challenges to the textile, clothing, and footwear industries. Companies, brands, and designers fight for their survival. Experts predict a big recession and prolonged recovery of the fashion system; according to the latest expert predictions, investments in the brand portfolio and image, incorporation of sustainability and transparency, investments in digital abilities and tools. To reduce the companies' impact as much as possible, professional organizations and governments support textile and garment industry companies with different initiatives and present diverse COVID-19 recovery strategy for the textile and apparel industry. These initiatives focus on building a strong European textile alliance and focus on the public, private partnerships (PPPs) at the EU level for accelerating the research, innovation, pilot testing, and demonstration in critical areas, like digital manufacturing and supply chains. [11]

[11] Also: Ukraine, Croatia and Bulgaria.

REFERENCES

[1] L. Hunt, “Hoisington Management report,” [Online]. Available: https://hoisington.com/pdf/HIM2020Q2NP.pdf. [Accessed 2. November 2020.].

[2] D. Emese, “Most az ördög sem visel Pradát: a divatipart is kiütötte a koronavírus,” 1. April 2020. [Online]. Available: https://hvg.hu/360/20200401_A_divatiparra_is_hosszan_es_nagyot_ut_a_koronavirus. [Accessed 5. November 2020].

[3] A. Becker, “Asia's textile industry hit hard by COVID-19 downturn,” 21. Octobre 2020.. [Online]. Available: https://www.dw.com/en/asias-textile-industry-hit-hard-by-covid-19-downturn/a-55345713#:~:text=The%20impact%20of%20the%20coronavirus,to%20a%20new%20ILO%20report.&text=This%20is%20particularly%20dramatic%20in,large%20share%20of%20all%20exports. [Accessed 27. November 2020.].

[4] Apparel Coalition, „Weaving a better future: Rebulding a more sustainable fashion industry after Covid-19,” 2020. [Online]. Available: https://apparelcoalition.org/wp-content/uploads/2020/04/Weaving-a-Better-Future-Covid-19-BCG-SAC-Higg-Co-Report.pdf.

[5] BOF TEAM, “In the Face of a Global Crisis, What Is the Fashion Industry Doing?,” 25. March 2020.. [Online]. Available: https://www.businessoffashion.com/articles/global-markets/in-the-face-of-a-global-crisis-what-is-the-fashion-industry-doing. [Accessed 5. August 2020.].

[6] Bussiness of Fashion (BOF), „Coronavirus: The Analysis the Fashion Industry Needs,” 2020.. [Online]. Available: https://www.businessoffashion.com/articles/tags/topics/coronavirus. [Hozzáférés dátuma: October 2020.].

[7] C. Lieber, “The Fashion-Tech Tools Getting a Boost As Covid-19 Takes Hold,” 19. March 2020.. [Online]. Available: https://www.businessoffashion.com/articles/technology/the-fashion-tech-companies-getting-a-boost-as-covid-19-takes-hold. [Accessed 25. March 2020.].

[8] Euratex, “A COMPLETE RECOVERY IS STILL UNCERTAIN, DESPITE SOME POSITIVE SIGNALS – THE LATEST ECONOMIC DATA SHOW,” 21. December 2020.. [Online]. Available: https://euratex.eu/news/a-complete-recovery-is-still-uncertain-despite-some-positive-signals-the-latest-economic-data-show/. [Accessed 28. December 2020.].

[9] TMTE és MKSZ, “Felmérés a hazai könnyűipar elsősorban a textil és ruházati szektor érintettségéről a koronavírus járvány kapcsán,” 6. Április 2020.. [Online]. Available: 6.. [Accessed September 2020. 2020.].

[10] TMS - Market Intelligence, „Impact of coronavirus on Serbian textile industry,” 8. August 2020.. [Online]. Available: https://www.textilemedia.com/about-us/latest-news/impact-of-coronavirus-on-serbian-textile-industry/. [Hozzáférés dátuma: 17 November 2020.].

[11] EURATEX, „Euratex presents COVID-19 recovery strategy for textile and apparel industry,” 20. July 2020.. [Online]. Available: https://apparelresources.com/business-news/manufacturing/euratex-presents-covid-19-recovery-strategy-textile-apparel-industry/. [Hozzáférés dátuma: 7. September 2020.].

[12] The Guardian, „Garment workeris face destitution as Covid-19 closes factories,” 2020. [Online]. Available: https://www.theguardian.com/global-development/2020/mar/19/garment-workers-face-destitution-as-covid-19-closes-factories?fbclid=IwAR0oW08fm4RgBZciz5pzuDjY6zc_YnB25-4YR9T-0lg7G6p4J4DFQ9lvEWE. [Hozzáférés dátuma: 15. November 2020.].

THE LIST OF CORRESPONDING AUTHORS

Dr. Ákos Borbély
Institute of Media Technology, Rejtő Sándor Faculty of Light Industry and Environmental Engineering, Óbuda University
Doberdó Street 6. H-1034 Budapest, Hungary
Phone: +(36) (1) 6665961 E-mail: borbely.akos@rkk.uni-obuda.hu

Dr. Ágnes Bálint
Óbuda University
Doberdó Street 6. H-1034 Budapest, Hungary
Phone: +36303721342 E-mail: balint.agnes@uni-obuda.hu

Glória Bernvalner
Szent István University
Páter K. Street 1. H-2100 Gödöllő, Hungary
Phone: +36703624997 E-mail: missgloria86@gmail.com

Dr. Bernadett Gyarmati
Szent István University
Páter K. Street 1. H-2100 Gödöllő, Hungary
Phone: +491728287310 E-mail: bernadett.gyarmati@gmail.com

Dr. Edit Csanák
Óbuda University Rejtő Sándor Faculty of Light Industry and Environmental Engineering, Budapest, Hungary
Doberdó street 6, 1034 Budapest, Hungary
Phone: +36 30 6673639 E-mail: csanak.edit@rkk.uni-obuda.hu

Dr. Tamás Csiszér
Óbuda University
Bécsi út 96/b 1034 Budapest, Hungary
E-mail: csiszer.tamas@uni-obuda.hu

Dr. Gabriella Oroszlány
Óbuda University
Bécsi út 96/b 1034 Budapest, Hungary
E-mail: oroszlany.gabriella@uni-obuda.hu

Edina Kulcsár
Pannon University
Egyetem út 10 8200Veszprém, Hungary
E-mail: kulcsare@fmt.uni-pannon.hu

Zsolt Borka
Óbuda University
Bécsi út 96/b 1034 Budapest, Hungary
E-mail: borka.zsolt@uni-obuda.hu

Dr. Eszter Kormány
Óbuda University
Bécsi út 96/b 1034 Budapest, Hungary
E-mail: kormany.eszter@uni-obuda.hu

Dr. Tibor Gregász PhD
Institute of Media Technology and Light Industry, Rejtő Sándor Faculty of Light Industry and Environmental Engineering, Óbuda University
Doberdó str. 6. H-1034, Budapest, HUNGARY
E-mail: gregasz.tibor@uni-obuda.hu

Veronika Pál
Institute of Media Technology and Light Industry, Rejtő Sándor Faculty of Light Industry and Environmental Engineering, Óbuda University
The full title of the Institution
Doberdó str. 6. H-1034, Budapest, HUNGARY
E-mail: palveronika.hu@gmail.com

Vera Göndör
Institute of Media Technology and Light Industry, Rejtő Sándor Faculty of Light Industry and Environmental Engineering, Óbuda University
The full title of the Institution
Doberdó str. 6. H-1034, Budapest, HUNGARY Street, ZIP-code City, Country
E-mail: gondor.vera@uni-obuda.hu

Dr. Ineta Nemeš
Technical Faculty “Mihajlo Pupin” Zrenjanin, University of Novi Sad, Department of Textile Engineering
Đure Đakovića бб, Zrenjanin 23000, Szerbia
E-mail: inetavil@gmail.com

Anita Sós
Department of International Management, Faculty of Foreign Trade, Budapest University of Economics

E-mail: sanitacz@gmail.com

Óbuda University
Integrált Tudományok Szakkollégiuma

ISBN 978-963-449-230-6